2-P
mix

Technical Report RSC-15

AERIAL 8-14 MICRON IMAGERY APPLIED TO MAPPING THERMAL EFFECT MIXING BOUNDARIES

by

Norman Gray Foster

August 1970

supported by

National Aeronautics and Space Administration

NGL-44-001-001

TEXAS A&M UNIVERSITY
REMOTE SENSING CENTER
COLLEGE STATION, TEXAS

AERIAL 8-14 MICRON IMAGERY APPLIED TO MAPPING THERMAL EFFECT MIXING BOUNDARIES

A Thesis

by

NORMAN GRAY FOSTER

Submitted to the Graduate College of
Texas A&M University in
partial fulfillment of the requirement for the degree of

MASTER OF SCIENCE

August 1970

Major Subject: INTERDISCIPLINARY ENGINEERING

ABSTRACT

Aerial 8-14 Micron Imagery Applied to Mapping Thermal Effect Mixing Boundaries. (August 1970)

Norman Gray Foster, B.M.E., North Carolina State College; M.S., Texas A&M University

Directed by: Dr. John W. Rouse, Jr.

An experiment was performed which appears to have some significance toward remotely monitoring thermal effect mixing boundaries within industrial coolant waters. The investigation was limited to determining water temperatures and calculating a steady-state energy balance of a fossil-fueled power plant effluent both from airborne imagery and from ground observations, and the comparison of the two calculations. The results enhance the practical applications of remote imagery to aquatic ecology studies.

Airborne 8-14 micron wavelength imagery was obtained over discrete locations along heated water effluent canals, coincident with subsurface water temperature measurements at the same locations. Water temperature and calculated heat exchange between the

canal water and the atmosphere were compared, using ground measurements and photo-interpreted measurements from the airborne data.

Results show that gross photointerpretation techniques can delineate water temperatures within five percent.

ACKNOWLEDGEMENT

Sincere appreciation is herewith expressed to my committee chairman, Dr. John W. Rouse, Jr., and to Dr. George L. Huebner, Jr. and Dr. Robert D. Turpin for the advice, guidance, and many hours of assistance through the course of this study.

The experiment airborne data was collected and reduced by the National Aeronautics and Space Administration, Manned Spacecraft Center, and sincere thanks are expressed to Robert O. Piland, Edward O. Zeitler, Joe Algranti, Larry Gaventa, Rose Ann Albrizio, Jerry Cobb and Frank Newman for this action.

Gratitude is also expressed to Leo Monford, Paul Vavra, Ike Eikemeir, and Richard R. Richards of the Manned Spacecraft Center instrumentation organizations for developing, calibrating, and making available the ground truth sensor, and to Chester Lloyd for assistance during the RS-14 instrument verification.

TABLE OF CONTENTS

LIST OF TABLES

LIST OF FIGURES

Figure | Page

CHAPTER I

INTRODUCTION

1.1 Summary

The literature records that the addition of thermal energy to natural water bodies results in positive changes to the water ecology and may produce contaminated products to man. Many ecologists consider temperature the primary control of life on earth. Heating of the rivers, estuaries, and lake waters due to industrial cooling is thought to threaten aquatic species, as they cannot adjust to abnormally abrupt changes. Water above 93 degrees Fahrenheit is believed unhabitable for fishes natural to this country. It is anticipated that this limit may be exceeded in many U.S. rivers.

The principal contributor of this waste heat is the electric power industry. Presently about 60 trillion gallons of water are used annually in the United States for industrial cooling, of which about 40 trillion are

---

The citations on the following pages follow the style of the Proceedings of IEEE.

used by the electric power industry. Thermal electric plants heat coolant water 12-13 degrees Fahrenheit. Nuclear-fired plants require 60 percent more coolant than the fossil facilities, and are estimated to require disposal of 20 trillion BTU's per day by the year 2000. Should the electric automobile or other battery powered public transportation be exploited within the next 30 years, this figure could increase significantly. Even without consideration of such transportation, nuclear generating facilities will require, by the year 2000, one-third of the daily fresh-water run-off in the United States--an increase of 240 percent over today's quantity.

Few gross studies have been conducted concerning the effects of thermal addition to water, however, the known physical changes to the water by thermal addition is causing an ever-increasing public concern over the management of natural water bodies for industrial heat sinks. Beneficial uses of the waste heat, such as the evaporating of seawater in desalination plants, and sea-farming, have not advanced to the degree of economic feasibility.

Increased public concern of this thermal effect may

well result in an increased need for data collection. Presently, the secondary effects are capable of being monitored with instruments recording within the visible portion of the spectrum. Primary thermal patterns are usually recorded within the 8-14 micron wavelength region because of minimum errors due to atmospheric contribution.

It is considered that the recording of thermal effect in water requires verification by field work and a broad overview of the water surface that is best achieved from aerial 8-14 micron imagery. It is also considered by those investigating the monitoring of thermal effect that a more positive method for differentiation of the boundaries of mixing zone should become available for use. This research was designed to test the application of an airborn technique for this purpose.

Presently there is sparse application of airborne thermal imagery to the delineation of the thermal mixing zones in natural water bodies. The question of what the patterns on the imagery actually represent relative to the subsurface thermal conditions is yet to be answered. Wind across the water surface could move warm water over

the surface of an area where the environment of the bottom ecology is cold water, and vice versa. Emissivities of the water surfaces may vary due to many physical changes which conceivably could result in thermal imagery not representative of the subsurface conditions. However, as with any form of data gathering, there are optimum and less optimum conditions that govern the specific technique to be used. It appears then that thermal imagery could be obtained when conditions of weather, tide, and surface heat flow are near optimum, and that the results could represent the subsurface water conditions to a gross degree that would be acceptable to the ecologist.

The experiment associated with this research is an attempt to gain information that would result in increased confidence and use of thermal imagery by those investigators concerned with monitoring the effects of industrial coolant water. The experiment was confined to interpreting aerial 8-14 micron imagery of the effluents from a fossil-fueled electric generating plant, located on a somewhat typical water body, relative to the energy

exchange also calculated from subsurface thermic information.

Results of the research show that the interpretation of airborne thermal imagery is in agreement with the ground measurements within 5 percent. The study also concludes that a similar controlled experiment should be conducted in the same general area to further establish the synoptic photo interpretation technique for zone differentiation over a large natural bay.

1.2 Scope of the Thermal Effect Problem

Cold-blooded aquatic animals can adapt to the slow seasonal temperature changes, but are very sensitive to thermal shock or abrupt temperature differences. The ecologists are, therefore, very concerned about the addition of heat to natural waters by man's activities, which could conceivably threaten aquatic life within the next thirty years (5).

The calefaction of U.S. waters by electric power plants is certain to increase as the power industry meets the rising national demand for electricity. The generating capacity of power plants in the continental U.S. is

estimated to have been 315,000 megawatts at the end of 1969 and is expected to reach 576,000 megawatts by 1980. Nearly 1.5 billion megawatt-hours of electric power was produced in 1969; the Edison Institute forecast an output close to three billion megawatt-hours in 1980 and between six and ten billion megawatt-hours by the year 2000 (48).

The average daily natural runoff of water in the continental U.S. is about 1.2 trillion gallons. About 10 percent of this amount is used for cooling the condensers in power plants. These plants, both fossil fueled and nuclear, are rapidly growing in number. A forecast shows that more than 200 billion gallons of cooling water daily will be required by 1980, and 600 billion gallons, or 50 percent of all the available freshwater runoff, by the year 2000 (36) (1) (35) (48). What has aroused ecologists is the ninefold expansion of electric power production that is in prospect with the increasing construction of large generating plants fueled by nuclear fuel. They release about 60 percent more energy than the fossil-fuel plants, and this energy is released as heat to condenser cooling water. During

1968 the Atomic Energy Commission reported that there were:

Military power plants and specialized facilities

15 operational nuclear power plants

31 power plants under construction

42 power plants under review or awaiting licensing decisions

14 power plants on order for which permits have not yet been applied

100 additional licensed nuclear reactors and facilities

An estimate is that by the year 2000 the electric power industry will require the disposal of about 20 million BTU's per day in this country.

Thermal cooling is a largely non-consumptive use of water; most of the surface water used for cooling returns to the lake or stream from which it came, carrying with it the heat acquired in the course of its use. The Federal Water Pollution Control Administration has declared that waters above 93 degrees Fahrenheit are essentially uninhabitable for fishes natural to this country. Many southern U.S. rivers already reach a temperature of 90 degrees or more in the summer through

natural heating alone. The waste heat from a single power plant of 1000 megawatts may raise the temperature of a river carrying a flow of 3000 cubic feet per second by as much as ten degrees, and a number of industries and power plants could likely be constructed on the banks of a single river (47).

1.3 Effects of Warming Natural Waters

Information in the open literature is very sparse concerning the effects of warming natural water bodies. Definite cases of detrimental effects are not available, however due to increasing public interest many ecologists are monitoring heated effluents for possible changes. The electric power industry finances many of these studies.

The general effects from the heating of water are known. The warming of water increases its capacity to maintain certain elements in solution. Some finfish and shellfish are natural concentrators of certain of these elements, and it follows that some of the edible marine life living in heated coolant water discharge areas may

either become more nutritious, or possibly become unfit for human consumption.

The addition of heat has definite effects on the physical characteristics of water and could affect the subsequent uses of the water. The heating of water accelerates biological activity which in turn speeds removal of dissolved oxygen, nutrient chemicals, and other substances which are required for normal aerobic life processes. If biological processes continue until the dissolved oxygen is diminished, organisms in bottom mud may stimulate thermogenesis, adding more heat to the water. Through this process, the initial addition of thermal energy to water could conceivably result in contamination (29) (37).

1.4 Purpose of the Study

Little research has been expended toward putting the hot water to use for the economy; it appears, however, that public pressures are leading to increased studies and possible near-time applications for this vast amount of energy.

The question concerning what should be done about

the thermal problem has not yet been answered. Unless the population is stabilized, demand for electric power will continue to increase and more waste heat will become available. Meanwhile, to avoid possible damage to our aquatic life, plans for thermal plants should hinge on ecological studies that map existing conditions and predict areas of special vulnerability.

The waste heat from thermal plants could conceivably be put to profitable use. Most of the ideas advanced so far have proven impractical. One of the most promising uses would be to use the energy to evaporate sea-water in desalination operations; another would be to use the heat in a controlled manner for sea-farming operations. The growing season of certain marine life could be extended in warm water and growth rate could be promoted because of the heat speeding of body processes. There are tests being conducted in Scotland that show certain fish can be raised to market size faster in nuclear plant seawater effluent than in natural ocean water. Other possible uses for thermal energy to benefit the economy could include (4):

1. Heated public swimming areas
2. Water farming
3. Ice-free areas for waterfowl wintering
4. De-icing of inland waterways
5. Water quality improvement
6. Industrial and domestic uses, such as hydronic heating of homes and offices, and systems for keeping streets and highways free of ice and snow

At the moment, however, most of the waste heat must be released directly into the environment. No matter where it is released it will have some effect on the ecosystem. If it must be added to the water, several alternatives are available, the choice of which should depend on the ecological nature of the receiving body of water. A discharge method producing least harm to one body of water might produce more harm to another (4).

1.5 Scope of this Thesis

Chapter I of this thesis was devoted to introducing the subject of thermal effect. The scope of the thermal effect problem was reviewed, and the general effects caused by warming natural waters were discussed. Chapter

I also addressed the question of why study the thermal problem.

Chapter II is a survey of the open literature concerning the thermal effect in natural water bodies. It contains a listing of available remote instruments that are presently used, a discussion of the role of photo interpretation concerning thermal studies, and brief outlines of the major studies now being conducted.

Chapter III is a description of the experiment conducted during this research. The experiment is summarized, the general site where the experiment was performed is reviewed, and the specific test area is discussed in detail. The ground truth equipment and the aircraft overflight and sensor are also reviewed.

Chapter IV is devoted to the results of the experiment. The airborne data is displayed and reviewed, and the data reduction procedures are explained.

Chapter V contains conclusions drawn from the data, and the research is summarized. Recommendations for further research are also included.

CHAPTER II

BACKGROUND

2.1 Remote Instruments Used for Thermal Studies

For thermal studies, there are several remote sensing instruments usable by the photo interpreter. A listing would include the following that record in the visible, infrared, and microwave portions of the spectrum:

Visible: Metric cameras
Panoramic cameras
Multiband synoptic cameras
Ultra-high resolution cameras
Multiband imagers

Infrared: Near infrared cameras
Infrared imagers
Multiband infrared imagers
Infrared radiometers

Other possible instruments:
Infrared spectrometers
Radar imagers
Passive microwave imagers
Passive microwave radiometers

Although camera systems are more common and have the advantage of high resolution and economy, they are

confined to be used during fair, sunny weather. In the past several years much progress has been made in developing thermal infrared sensing and its application to the mapping of surface phenomenon. Infrared radiation is generated by dynamic movements of the atoms and molecules within any material whose temperature is above absolute zero, consequently, practically everything in man's surroundings, and man himself, radiates energy in the infrared portion of the electromagnetic spectrum. The generally accepted infrared spectrum lies between the wavelengths of 0.72 and 1000 microns (23) (28).

Infrared instruments suitable for monitoring heated coolant water are passive systems which have a very short time-constant to respond to small temperature changes in the water mass, and to the forward motion of the aircraft. If possible, the instrument should permit indication of boundary zones between heated and cool waters. The temperature response of the instrument should include the spectral region extending from 9.3 microns to 10.8 microns which corresponds to the critical temperature range.

Presently, remote surface temperature measurements

of objects can be made with a fair degree of accuracy from the air using various types of available infrared sensors. One type of aerial infrared sensor reportedly has an accuracy of .006 degree Centigrade from an altitude of several thousand feet (29); imaging systems now in practical use, however, do not have this capability.

2.2 Photointerpretation Concerning Thermal Studies

Perhaps in no other way than photographic interpretation can a vast area be studied so rapidly. Laboratory and field analysis methods cannot be replaced with photographic interpretation techniques, however they can be greatly assisted and the specific areas requiring detail effort can more quickly be identified and isolated. The associated reduction in field work saves time and money that can be applied to confirming laboratory analysis, and for solving the problems that may exist (19).

Photographic analysis of water quality requires application of information concerning the selective spectral energy absorption, transmission, and reflection properties of the water body being examined. Minor

tonal differences in the recorded images may indicate significant differences in water quality (19).

Multispectral aerial photography can be manipulated to enhance, by radical color differences, minute changes in the spectral reflectance of water. Thermal activities are usually indicated in the differences of the images obtained, therefore aquatic patterns can sometimes be studied and evaluated using this technique (26).

Infrared sensed data provides supplemental information to that obtained by aerial photography and may be used to obtain information at night or at other times when aerial photography cannot be taken. The interpreter, however, must take into consideration the environmental conditions that prevailed during the time the infrared imagery was obtained (23).

Several problems have been encountered by the photo-interpreter in studies of thermal effect in natural water bodies. A need has been voiced for better differentiation of the boundaries of mixing zones (39), which is the object of the experiment associated with this research. Studies indicate that some of the most commonly used engineering formulas for forecasting diffusion and

dispersion of substances into flowing water may be in error by a factor of 6 to 10 if applied to natural streams (40). Photographic techniques are about the only methods available for determining such boundaries (29).

There are many more physical processes involved in producing infrared images than there are in producing photographs made in the visible reflected light region. All of these processes must be considered when analyzing the imagery. Analysis of IR imagery is complex and quantitative information about many of the processes must be available before analysis can be accomplished. With some knowledge of the physical processes involved, and correlative information, much can be extracted by the interpreter from imagery made in a single broad-wavelength band, even though no ground truth data is available. The interpretation of infrared imagery is a field full of potential value and is expanding as multi-channel imagery becomes more and more common (24).

Heat, at the levels present in heated cooland water, or in the receiving discharge areas, cannot be recorded using conventional photography. The temperature from about 30 degrees to 120 Fahrenheit consists of energy

which peaks in the range from about 9.3 to 10.8 microns in wavelength. This is the deep infrared region and is well beyond that which can be photographically recorded with cameras. Photographic imagery can be quite successfully recorded in the spectral region extending from the ultraviolet to the near infrared, the upper limit being at approximately 1.5 microns.

If one is to analyze thermal patterns in photographs, one must then analyze secondary information. That is, study the change in the image as induced by physical changes caused by heat rather than actually picturing the heat itself. A photographic monitoring system is preferred because of the advanced state of the art of photointerpretation. Use of image-forming infrared sensors, while offering several significant advantages, including discrete picturing of heated water masses, also offers some disadvantages. Most of the systems currently in use exhibit considerable geometric distortion and resolution well below that obtained in photography. Studies to date support the hypothesis that many thermal boundaries may be delineated by recording the significant secondary characteristics (29).

Many modern remote sensing techniques and studies are concerned with the development of high speed data collection and analysis by automatic means. Such systems are not yet readily available. The state-of-the-art instruments that are available for use produce images in forms common to natural surroundings. These pictures must then be interpreted by people. It appears that the image-interpreter will have a place in the economy for a long time, and his ability to extract real and pertinent information from data will help solve many of the problems man is creating for himself.

2.3 Current Thermal Studies

Many current studies have been conducted concerning remote sensing of the thermal environment and its associated effects. Some of these are as follows.

Thermal infrared mapping along the Michigan shore has shown a complex pattern of thermal surface gradients in the lake. The changes in temperature also produce changes in algae content (45).

The U.S. Geological Survey (USGS) has an estuarine remote sensing program to determine the feasibility of

using remote sensors for studying estuaries from aircraft or spacecraft platforms. One of the estuaries being studied is in the Delaware River. Preliminary remote sensed data of this estuary indicate that surface thermal variations of as small as one degree Centigrade and spatial variations as small as 100 feet can be detected by aircraft-mounted imaging systems. These are the most subtle contrasts that have been readily detected. Larger phenomena have been detected that have greater thermal contrasts. One such is the thermal effluents from electric-power generating plants which may have spatial dimensions of one-half mile and thermal contrasts of up to ten Centigrade degrees. It appears that the general circulation of some estuaries and bays could be monitored from spacecraft during some seasons of the year when thermal or color contrasts are present (42).

Another USGS study concerns heated effluents. Thermal characteristics of bodies of water are used to identify surface current patterns and distribution of heated effluent from power plants. Thermal imagery is a standard technique used in these studies. Evaluation of

thermal imagery obtained for this study is not complete, however, the following generalizations have been made. (1) Temperatures measured with a radiometer at 500 feet of elevation were one to two degrees cooler than surface temperature. (2) Differences in radiometric quantities of water and marsh plant communities may be correlated with gray tone on the imagery (44).

A study of Biscayne Bay has been conducted by Mahlon G. Kelly with data collected before and after a thermonuclear power plant become operational at Turkey Point. Although there are not many man-made effects in the portion of Biscayne Bay studied, changes due to man's activities were evident in the data. This is in relation to the natural distribution of bottom cover. Aerial studies of these effects proved to be of considerable interest to local workers and agencies (34).

CHAPTER III

THE EXPERIMENT

3.1 Summary

An experiment was performed which appears to have some significance toward remotely monitoring thermal mixing boundaries within industrial coolant waters. The investigation was limited to determining an energy balance of a fossil-fueled power plant effluent both from airborne imagery and from ground observations, and the comparison of the two methods. The results enhance the practical applications of remote imagery to aquatic ecology studies.

In applying airborne thermal imagery to the delineation of mixing zones, two steps are considered: first, evaluating the gross differences that may exist between using airborne imagery and ground data for energy balance determinations of a reasonably controlled water body, and secondly the evaluation of gross differences that may exist between using airborne imagery and subsurface thermic data for depicting the subsurface mixing

zones in natural water bodies. The experiment described herein was intended to accomplish the first of these steps; the results serve to document the gross adequacy of the airborne technique, and the physical conditions that may constrain the use of thermal imagery for this purpose.

The experiment utilized the capabilities within the NASA Earth Resources Program at the Manned Spacecraft Center, Houston, Texas. The prime airborne sensor used for recording the imagery was a calibrated thermal infrared detecting set designated as an RS-14. The RS-14 is mounted in the forward underneath side of an Orion NP3-A aircraft, which is also equipped with other sensors and supporting equipment.

The water selected for study is contained within two canals, each approximately four miles in length, which transport effluent from a power plant to a brackish natural water lake. During overflight of the RS-14 scanner, ground temperature measurements of the canal water at locations mutually available to both methods of data collection were recorded. Air and ground

photography were also recorded during the actual experiment for documentary purposes.

3.2 The Site

3.2.1 General surroundings

The area around Clear Lake, Texas, is an ideal location for conducting thermal effect studies in natural waters. The latitude of the area is near that of other southern rivers and estuaries that may be affected more by the ever-increasing industrial cooling problem. Also due to latitude, there is a low tide range in the area which allows the physical contribution of the tide to be more easily evaluated. Bottom ecology in the area is of great importance due to the multi-million dollar shrimp, oyster, crab, and finfish industry which is sensitive to water temperature behavior. The physical characteristics of Clear Lake-Galveston/Trinity Bay are very similar to other bay areas of industrial, economic, and private importance along the coast of California, Texas, Louisiana, Mississippi, and Florida. Additionally, industrial

plants

plants and their effluents, in the Clear Lake area, are also typical of those in other bay areas.

The Clear Lake area began a rapid growth in 1961 and presently more than 55,000 people live and work in the area. More than eighty aerospace firms are in the area, and a large industrial complex known as Bayport is well underway there. Bayport now contains fifteen chemical companies located on 8750 acres, and its own man-made seaport. Figure 3-1 is a high-altitude photograph of the Clear Lake area which shows the natural lake and man-made improvements around the lake. Figure 3-2 is an interpretive key to this photograph and will be referred to several times during the remaining text.

3.2.2 Test area

A medium-sized fossil-fueled power plant is located near the west end of Clear Lake, as shown in Figure 3-2. The plant is composed of three boilers, or steam generators; three alternators; and three condensers, or heat exchangers, where the used steam is condensed back to water.

Figure 3-1. Aerial view of test area.

This is a view of Clear Lake, Texas, and the surrounding area. Galveston Bay is at the bottom, Clear Lake is at the bottom center, NASA is immediately above Clear Lake, the local power plant is in the upper-left section of the picture, and the two heated water effluent canals flow from the power plant to locations on either side of the lake. Figure 3-2 is a detailed interpretive key to this photograph.

This picture was recorded at 60,000 feet from an RB57-F aircraft using a 9 inch format Zeiss metric camera having a 12 inch focal length lens. The scale is 1:60,000.

Figure 3-2. Graphic illustration of test area.

This is a detailed interpretive key to the photograph in Figure 3-1. The numbers along the canals are those of the ground truth station where subsurface water temperatures were recorded during the experiment. Some of the subsequent figures are detail photographs of these stations.

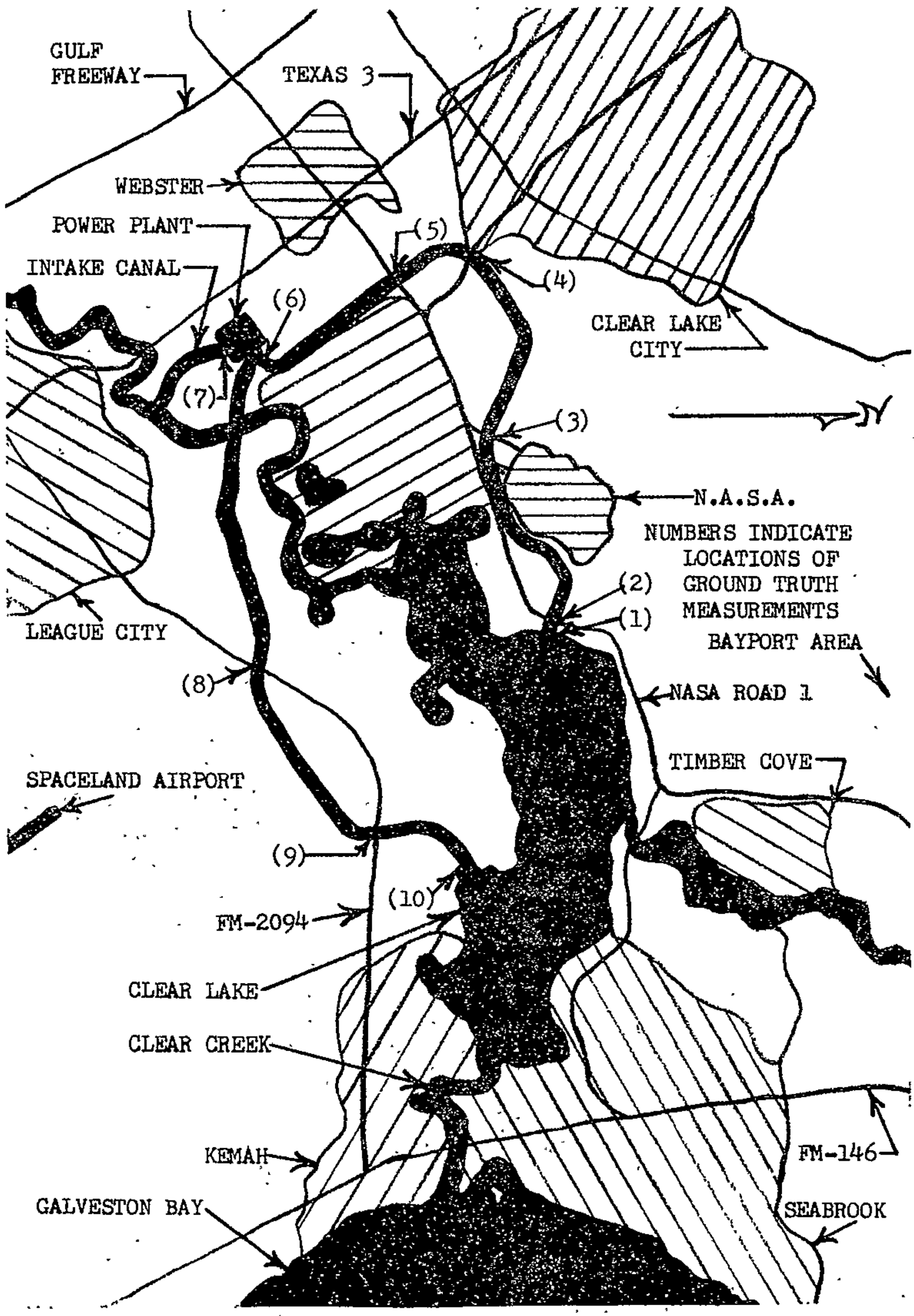
GULF FREEWAY
TEXAS 3
WEBSTER
POWER PLANT
INTAKE CANAL
(5)
(4)
(6)
(7)
CLEAR LAKE CITY
(3)
N.A.S.A.
NUMBERS INDICATE LOCATIONS OF GROUND TRUTH MEASUREMENTS
(2)
(1)
LEAGUE CITY
BAYPORT AREA
(8)
NASA ROAD 1
TIMBER COVE
SPACELAND AIRPORT
(9)
(10)
FM-2094
CLEAR LAKE
CLEAR CREEK
KEMAH
FM-146
GALVESTON BAY
SEABROOK

Two of the boilers and their associated alternators are capable of producing 115 megawatts of electrical power each, and the third unit can produce 350 megawatts. It is not uncommon for all three of these units to produce at their rated capacities on hot summer days when the humidity is high and residential air conditioners in the Clear Lake area are also functioning at their rated capacities. The power generating units operate on a conventional cycle with subcritical steam. Petroleum fuel is burned in the boilers where water is converted to steam at moderate pressures. The steam is piped to turbines where the thermal energy from the petroleum is extracted and converted to mechanical energy, or turning the shafts of the turbines. The shafts of the turbines are connected to alternators that produce electrical power for the local area.

After the steam passes through the turbines, it is still steam but of much lower pressure and temperature. This steam is to be reclaimed in the power-generating cycle, so it is passed through a condenser where it is cooled and transformed to water. The water is then pumped back into the boilers and the thermodynamic cycle

begins again. The condensers are cooled by pumping natural water through them. The water is extracted from a small intake canal that connects the plant with Clear Creek, indicated in Figure 3-2. After the water is used to cool and condense the steam, the water is higher in temperature than before.

The heated water flows from the three condensers into a small mixing pond, then divides into two canals. A schematic of this flow is shown in Figure 3-3. One of these canals flows initially northward. The canal is forty feet wide, five feet deep, and flows for a distance of 20,000 feet to where the water drops over a cataract, then into Clear Lake. The second canal flows initially southward from the power plant, and is 70 feet wide, five feet deep, and 21,000 feet in length.

Five locations along the North Canal were used as stations for determining ground truth temperature information during the experiment, and four along the South Canal. These specific locations were chosen because they were mutually accessible by automobile and from the air; they each were constrictions in the canal that created

Figure 3-3. Schematic of flow through power plant.

This is a schematic of the water flow through the electric power generating plant, and of the physical layout of the plant itself. Figure 3-12 is a pictorial view of this schematic.

Cool water flows from Clear Creek through an intake canal, and is pumped through the three condensers of the three generating units. The heated effluent water divides into the two north and south canals that carry the water into Clear Lake.

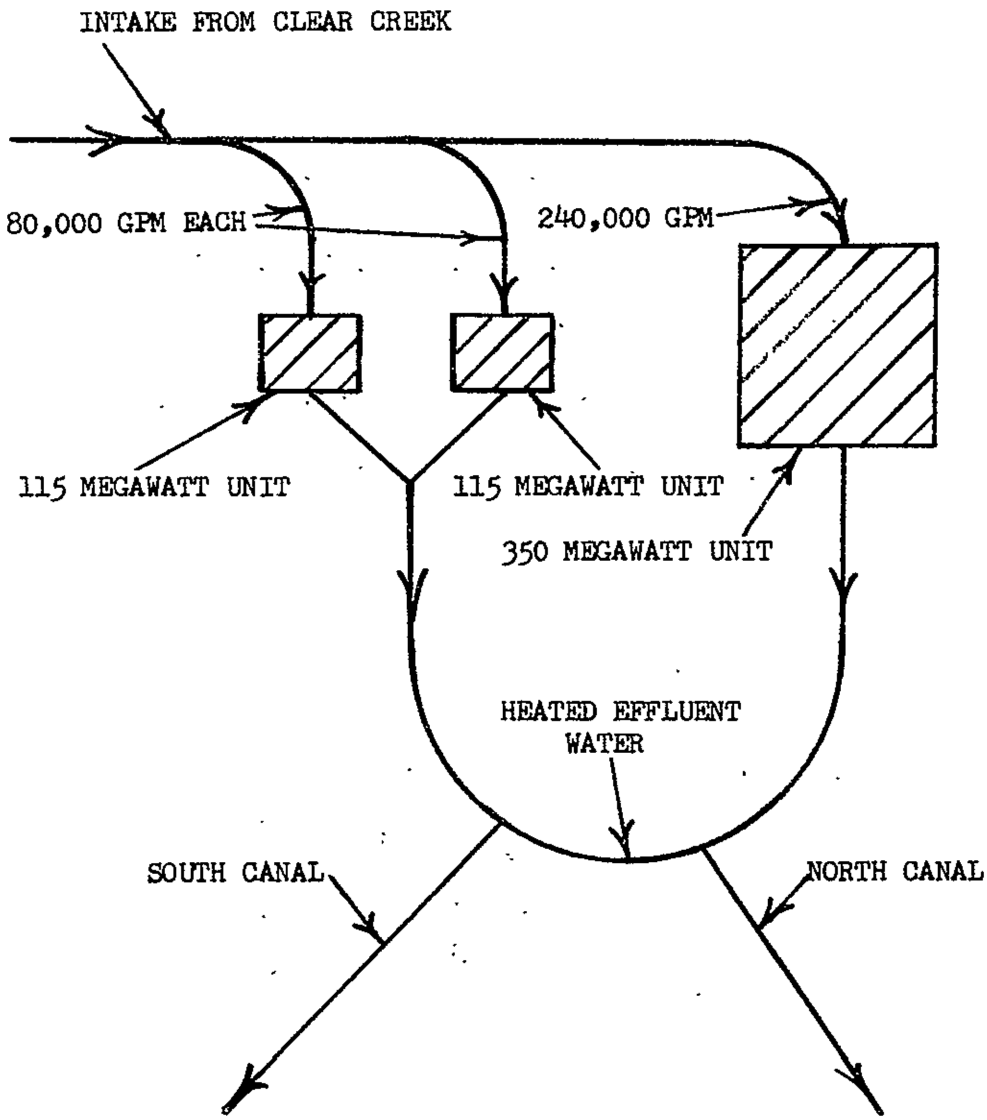
INTAKE FROM CLEAR CREEK
80,000 GPM EACH
240,000 GPM
115 MEGAWATT UNIT
115 MEGAWATT UNIT
350 MEGAWATT UNIT
HEATED EFFLUENT WATER
SOUTH CANAL
NORTH CANAL

violent mixing of the heated waters; and they were spaced reasonable distances apart along the length of the canal.

It was necessary that the locations where temperatures were to be recorded be readily accessible. The airborne measurements were planned to be conducted within a time span of one hour, therefore the ground measurements to coincide with the airborne measurements must of necessity be conducted as quickly as feasible. Prior to the experiment a versatile helicopter, shown in Figure 3-4, was used in surveying the canals from the air and in selecting the locations along the canals that would be mutual to air and ground transportation. Afterwards these locations were each studied on the ground for several days before the specific ground truth locations were finally fixed. The method of ground study used was to record subsurface water temperatures on a grid in the cross-section of the most violent flow. This flow was usually where the water emerged from concrete culverts that were underneath roadways, as illustrated in Figure 3-5. If the water was mixed sufficiently so that the temperature of the entire cross-sectional flow did not very more than one-tenth degree Fahrenheit, the location

Figure 3-4. Survey helicopter.

Numerous trips were made around the lengths of the two canals before finalizing the locations of the specific ground truth data stations. However, not until the versatility afforded by using a helicopter to survey the most likely areas could the final decisions be made.

The locations were to be mutually accessible from the ground and from a low-flying heavy aircraft, and to be areas of violent mixing of the canal water.


7

Figure 3-5. Typical ground station flow schematic.

This is a schematic showing the typical flow of canal water from concrete culverts under a roadway. Restrictions in the canals such as these caused mixing of the water and seemed to equalize the temperatures across the cross-section exiting from the culverts.

The dot pattern is representative of the grid used when determining the subsurface water temperature.

Figure 3-9 is a pictorial representation of this schematic.

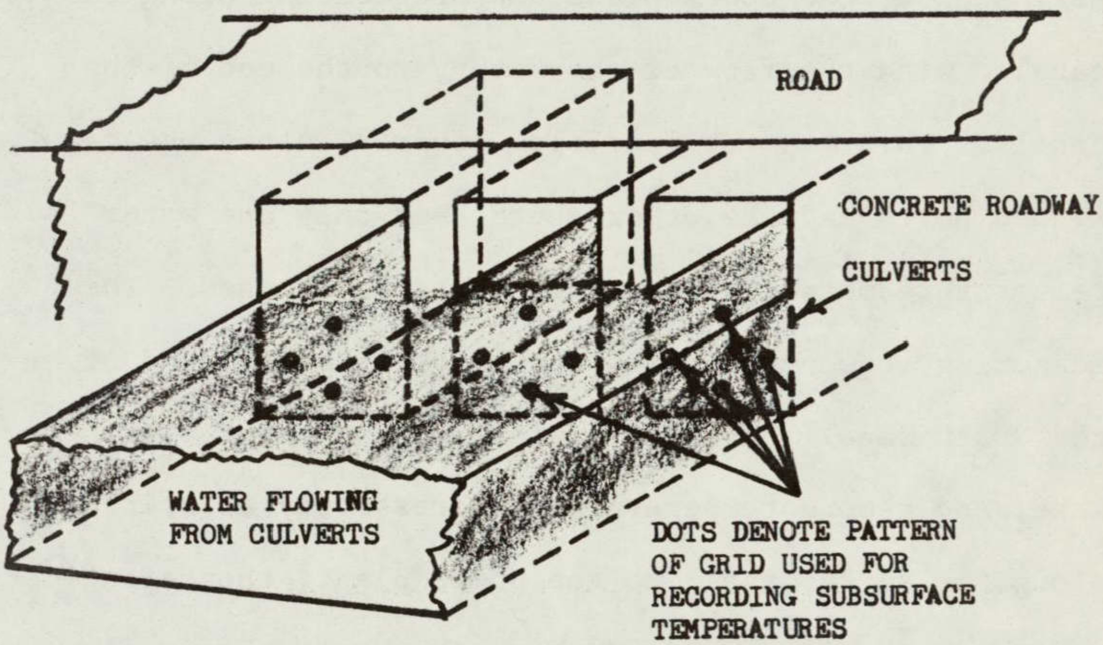
ROAD
CONCRETE ROADWAY
CULVERTS
WATER FLOWING
FROM CULVERTS
DOTS DENOTE PATTERN
OF GRID USED FOR
RECORDING SUBSURFACE
TEMPERATURES

was considered acceptable to obtain representative subsurface temperatures.

Also prior to the experiment, the sequence of recording the ground measurements was established. It was preferred that the temperatures be recorded at stations beginning at the power plant and progressing along the canals, with the flow of the water, to the end of the canals. This was not feasible, however, since one canal flowed north and the other south, and only one water temperature measuring instrument was to be used. The measuring sequence adopted was to begin at the end of the North Canal where the heated water entered Clear Lake, and record temperatures progressively at stations along the North Canal, to the power plant, then along the South Canal to the end where the heated water also entered Clear Lake. Rehearsing this sequence several times prior to the overflight resulted in a method of obtaining the water temperatures during a minimum elapsed time period. The specific ground locations were finalized and numbered in the order that they would be used during the experiment, with Station 1 being the outfall of the North Canal and Station 10, the last one, being

the outfall of the South Canal. Figure 3-2 also denotes the locations of these ten ground truth stations.

Stations No. 1 and 2 are pictures in Figure 3-6. Station No. 1 is below the cataract where the North Canal terminates at Clear Lake. Station No. 2 is above the cataract, at the outflow of the three culverts shown at the far left center of the picture.

Station No. 3 is shown near the top of Figure 3-7. It is located at the main gate of the Manned Spacecraft Center, where the canal water flows from culverts underneath the roadway. Station No. 4 is shown in Figures 3-8 and 3-9. The heated water at this location flows between a drainage canal and the four-lane El Camino Real in Clear Lake City. Although the culverts can be seen in the aerial view of Figure 3-8, Figure 3-9 is a close-up picture that better indicates the type of construction along the canals.

Station No. 5 is shown in Figure 3-10, and Figure 3-11 is a photograph from Station No. 5 showing the typical environment along the banks of the canals. Station No. 5 is where the heated water of the North Canal exits from culverts below NASA Road One. The violent mixing

Figure 3-6. Ground truth Stations No.1 and No. 2.

This is a view looking east of ground truth stations No. 1 and No. 2. Station No. 1 is below the cataract, known as the "Dragon's Teeth," where the heated effluent of the north canal enters Clear Lake. Station No. 2 is at the discharge of the culverts shown at center-left on the photograph. These stations are on federal-property at the Manned Spacecraft Center. Trees in the foreground are part of a pecan orchard that once belonged to the West Ranch. The object in the lower right corner is part of the helicopter structure.

Figure 3-7. Ground truth Station No. 3.

This is a view looking west containing ground truth Station No. 3. Station No. 3 is at the single bridge across the North Canal shown near the top of the picture. The main gate to NASA is immediately to the left of the bridge, and some of the parking lots of NASA are shown on the right side of the picture. The four lane road is NASA 1, and the complex of buildings on the left house aerospace companies. The North Canal is flowing in the direction from top to bottom of the picture.

Figure 3-8. Ground truth Station No. 4.

This is a helicopter view from 500 feet elevation looking west at ground truth Station No. 4. Station 4 is located on the immediate near side of the culverts between the roadway and the drainage ditch. The North Canal flows eastward here, from upper left to bottom right in the picture. The four-lane road is El Camino Real, the main entrance to Clear Lake City located off the right of the picture. The round structure at right is the Junior Achievement building in Clear Lake City.

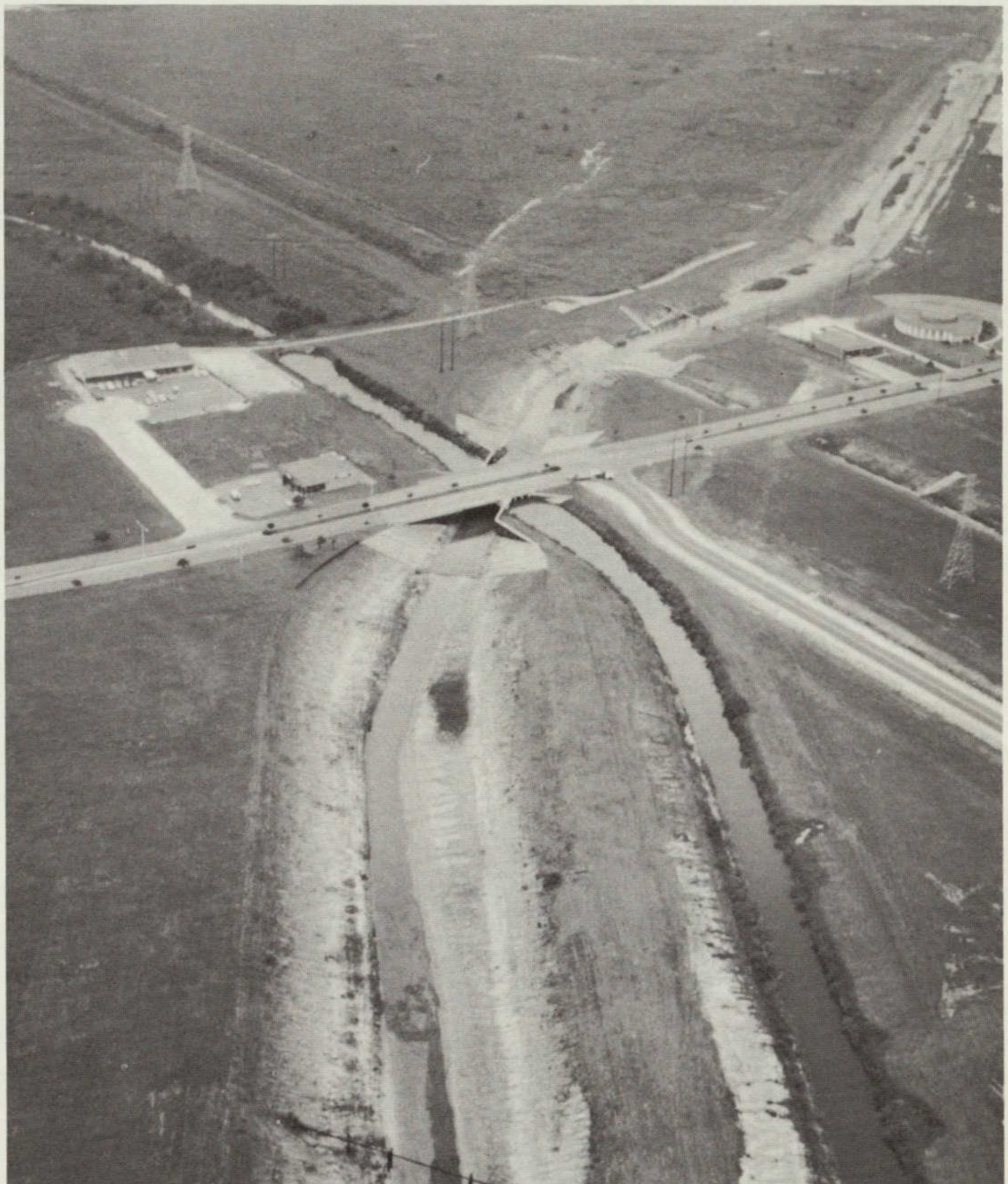

Figure 3-9. Close-up view of Station No. 4.

This is a view looking west at ground truth Station No. 4. Flow here is to the east, and the station is at the exits of the culverts. Figure 3-5 represents a typical station like this one.

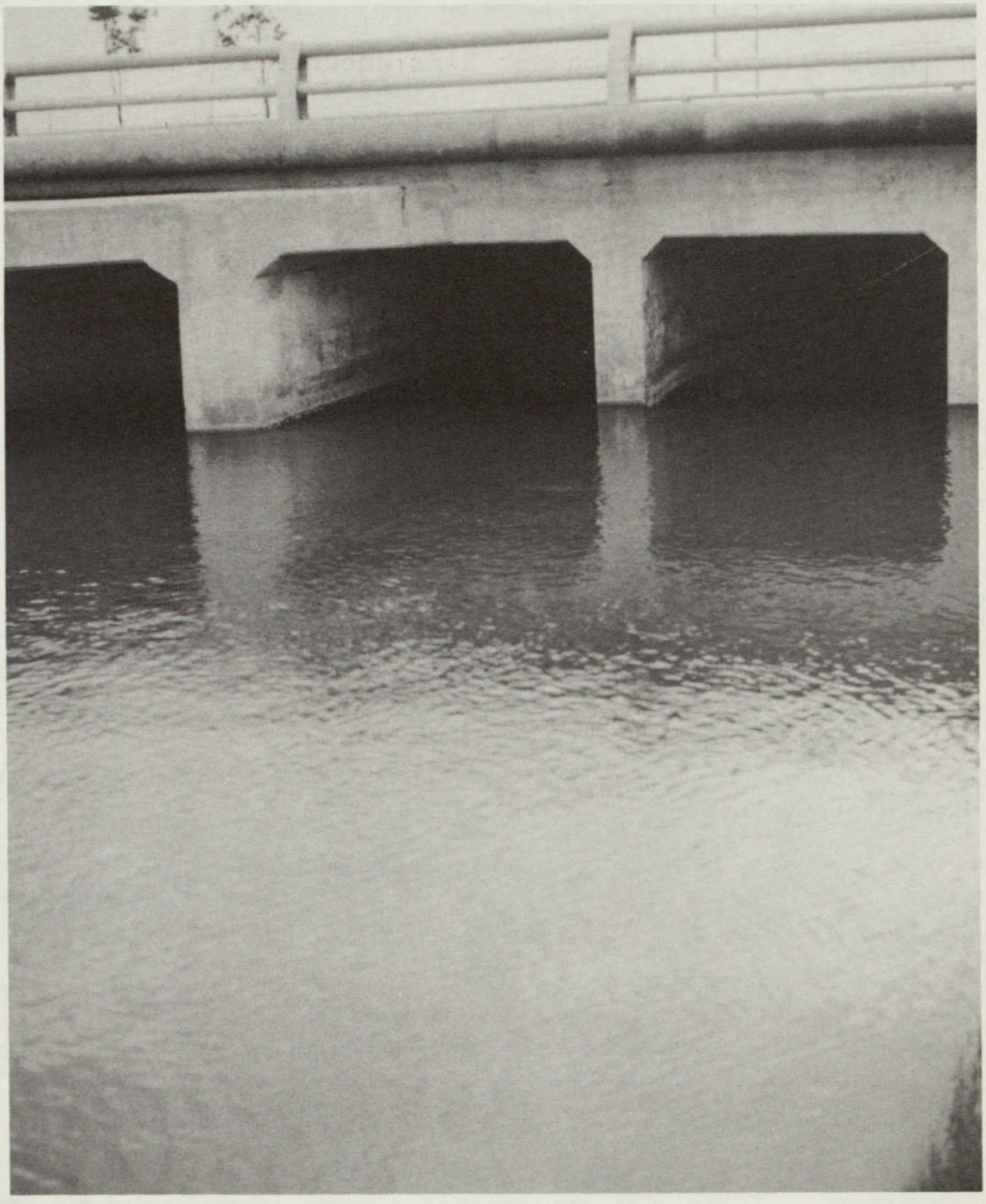

Figure 3-10. Ground truth Station No. 5.

Ground truth Station No. 5 is shown here. The top picture indicates the violent action of the flowing water, and the bottom shows a typical water temperature measurement being obtained. Station No. 5 is located where the North Canal crosses NASA Road 1, at the exit of the culverts. In the bottom picture, the flow is from left to right.

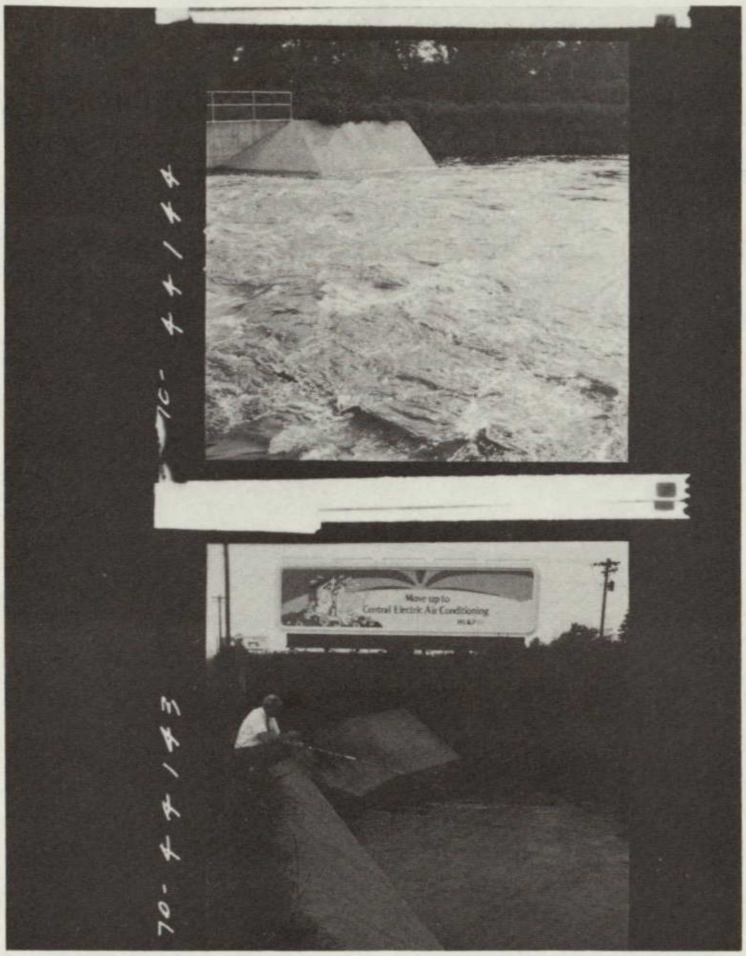
70-44/44
Move up to
Central Electric Air Conditioning
70-44/43

Figure 3-11. Effluent canal at Station No. 5.

This is a view looking north from Station No. 5, on the North Canal. Water at the bottom of the picture has exited from culverts beneath NASA Road 1, and is flowing northward. The healthy and abundant vegetation evident in this view is typical along the canals.

The canal turns east, to the right, at the far end of this view, and continues to Station No. 4.

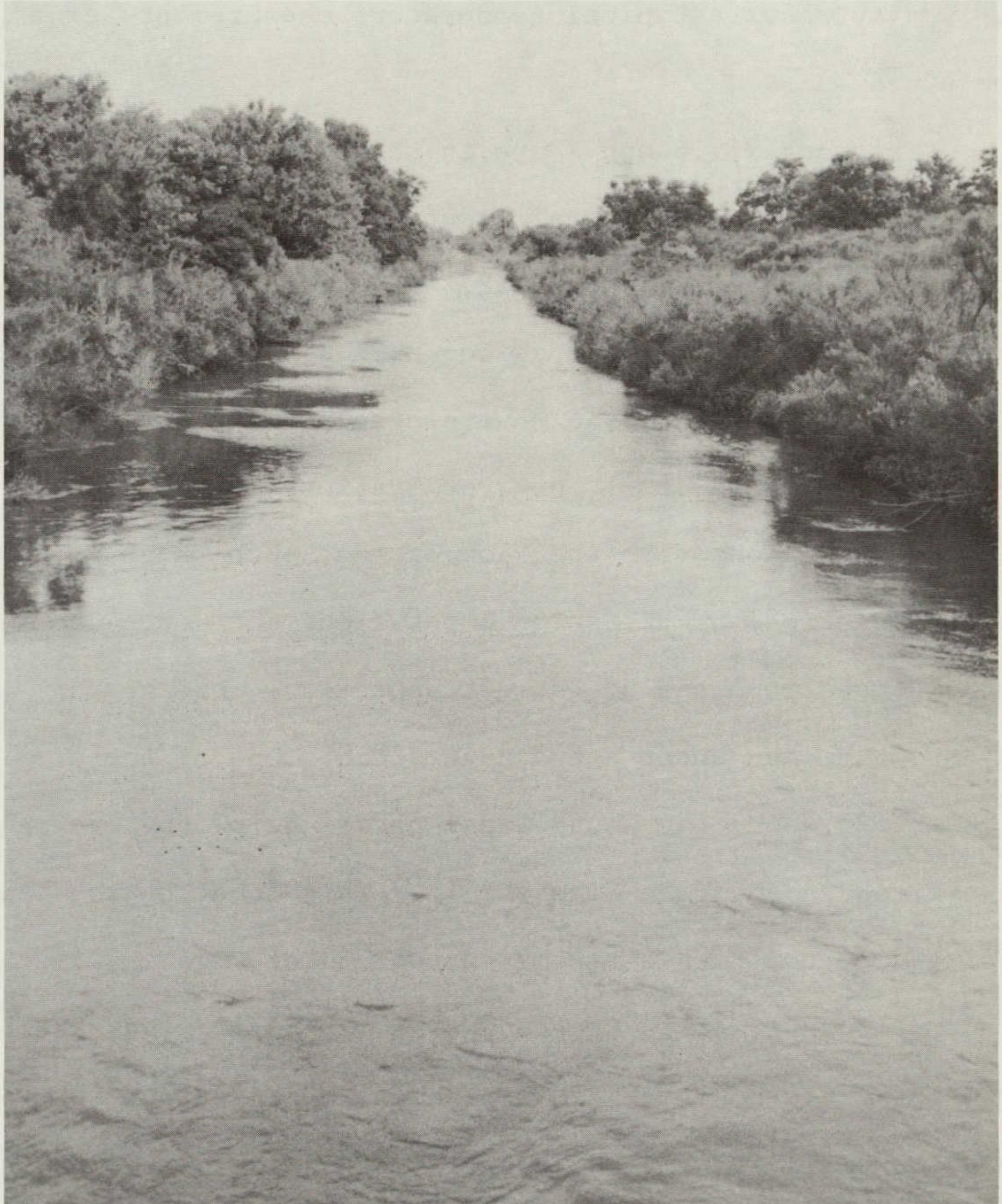

action of the water is evident in both figures. Figure 3-10 also shows a typical temperature measurement being obtained.

Stations No. 6 and 7 are at the power plant. Station No. 6 is the heated effluent as it emerges from the plant, as shown in Figure 3-12, and Station No. 7 is the intake to the power plant as shown in Figure 3-13. Stations No. 1 through No. 6 have progressed counter to the flow of the North Canal, however Stations No. 8, 9, and 10 progress along with the flow of the South Canal.

Downstream of the power plant along the South Canal at two locations the heated effluent flows underneath Clear Creek and under a drainage ditch. One of these locations, where the South Canal passes below the drainage ditch is shown in Figure 3-14. This location is also evident on the high-altitude photograph of Figure 3-1. Farther downstream is Station No. 8, shown in Figure 3-15, where the heated water flows beneath a bridge. At this station small fish may be seen living in the heated water, and near the canal crayfish shellfish seem to thrive.

Figure 3-15 is also typical of Station No. 9, being downstream along the South Canal from Station No. 8.

Figure 3-12. Aerial view of canals at power plant.

This is an aerial view looking west of the coolant water emerging from the power plant. The intake canal can also be seen at center-left in the picture. The metal structures at the termination of the intake canal are shown close-up in Figure 3-13, being the pumps that force the water through the condensers and into the canals.

The heated water emerges from the plant at two locations, the left source after cooling the condensers of the two 115 megawatt units and the right source after cooling the condenser of the 350 megawatt unit. Both sources mix together, as shown in the foreground of the picture, then the heated water divides and flows partly into the North Canal, bottom right of the picture, and into the South Canal, bottom left of the picture. The flow schematic of Figure 3-3 also illustrates this picture.

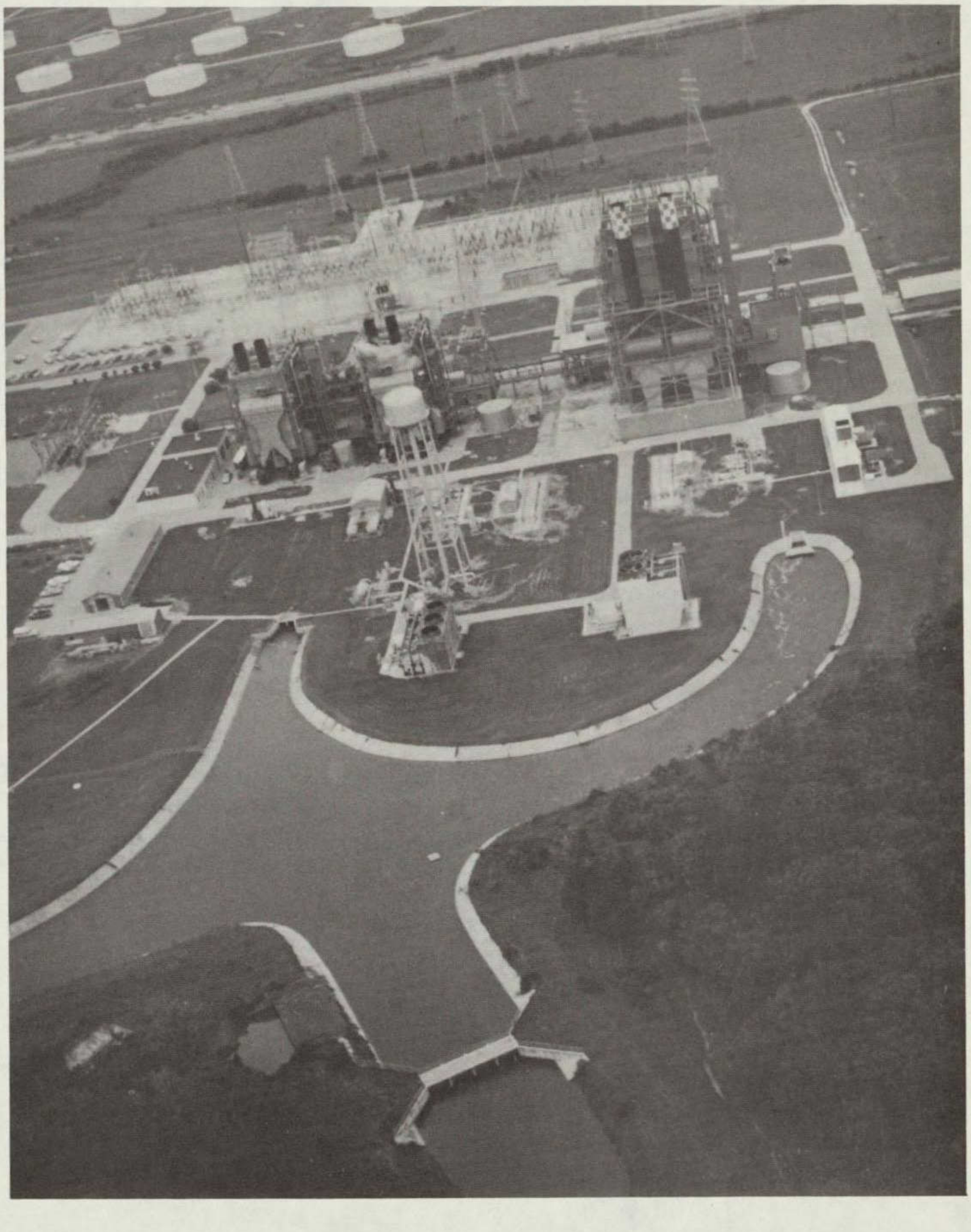

Figure 3-13. Grount truth Station No. 7.

Both of these views are of Station No. 7. The top view shows the termination of the intake canal between Clear Creek and the power plant. The large vertical pumps raise the water and force it through the three condensers of the power plant. The top view is of Station No. 7, and is the location where water enters the power plant.

The bottom picture is a close-up view of the pumps that move the coolant water from the intake canal through the power plant.

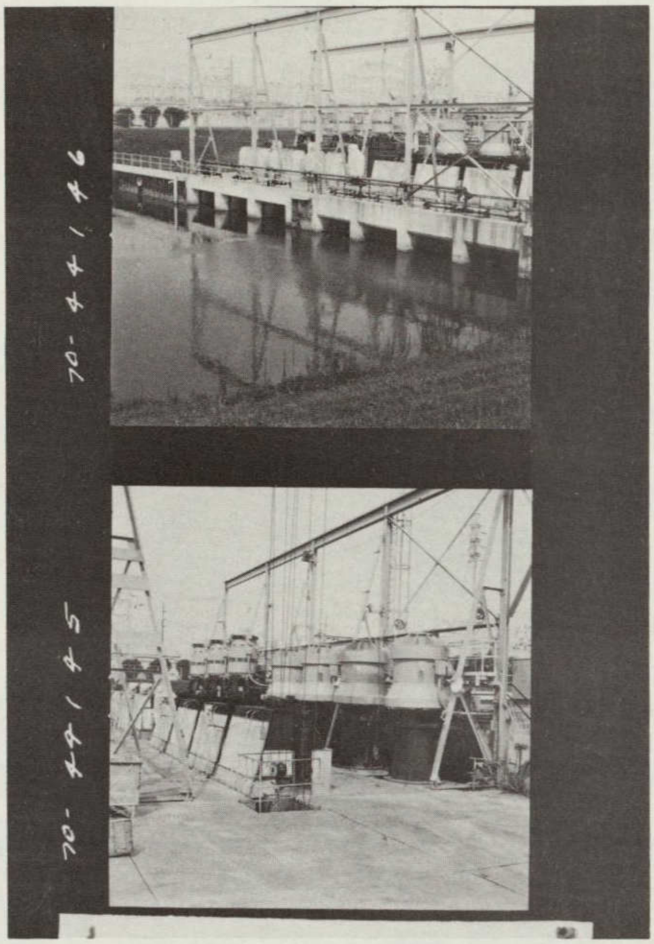
70-44146
70-44145

Figure 3-14. South Canal underpass of drainage ditch.

This is an aerial view looking north-east of the South Canal as it passes under the drainage ditch. The South Canal passes under other waters twice between the power plant and Station No. 8. The South Canal water is flowing from left to right in this picture, and the drainage water is flowing from bottom toward the top of the picture.

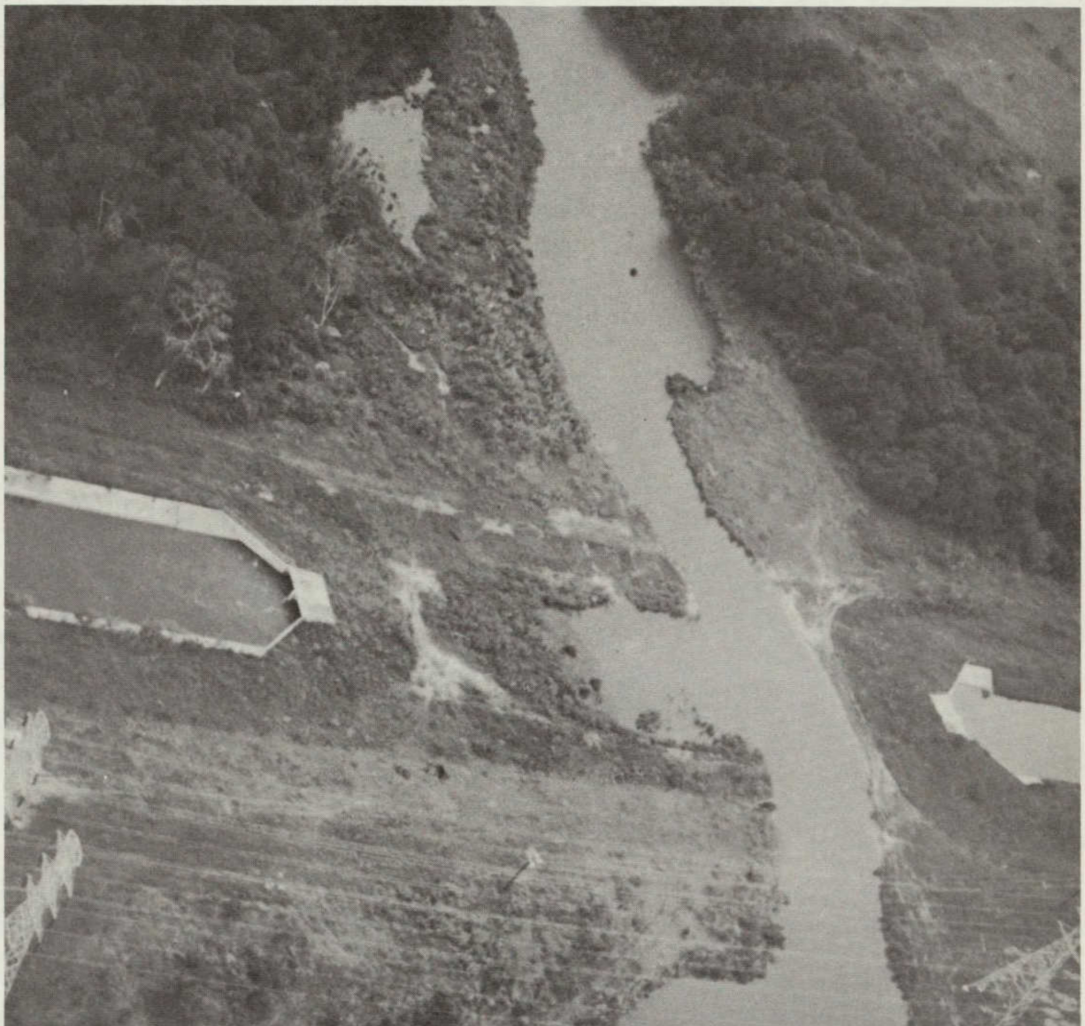

Figure 3-15. Ground truth Station No. 8.

This is a view of ground truth Station No. 8, where the South Canal flows under road FM-2094 near League City. This view is also very similar to Station No. 9, where the canal flows under the same road near the city of Kemah.

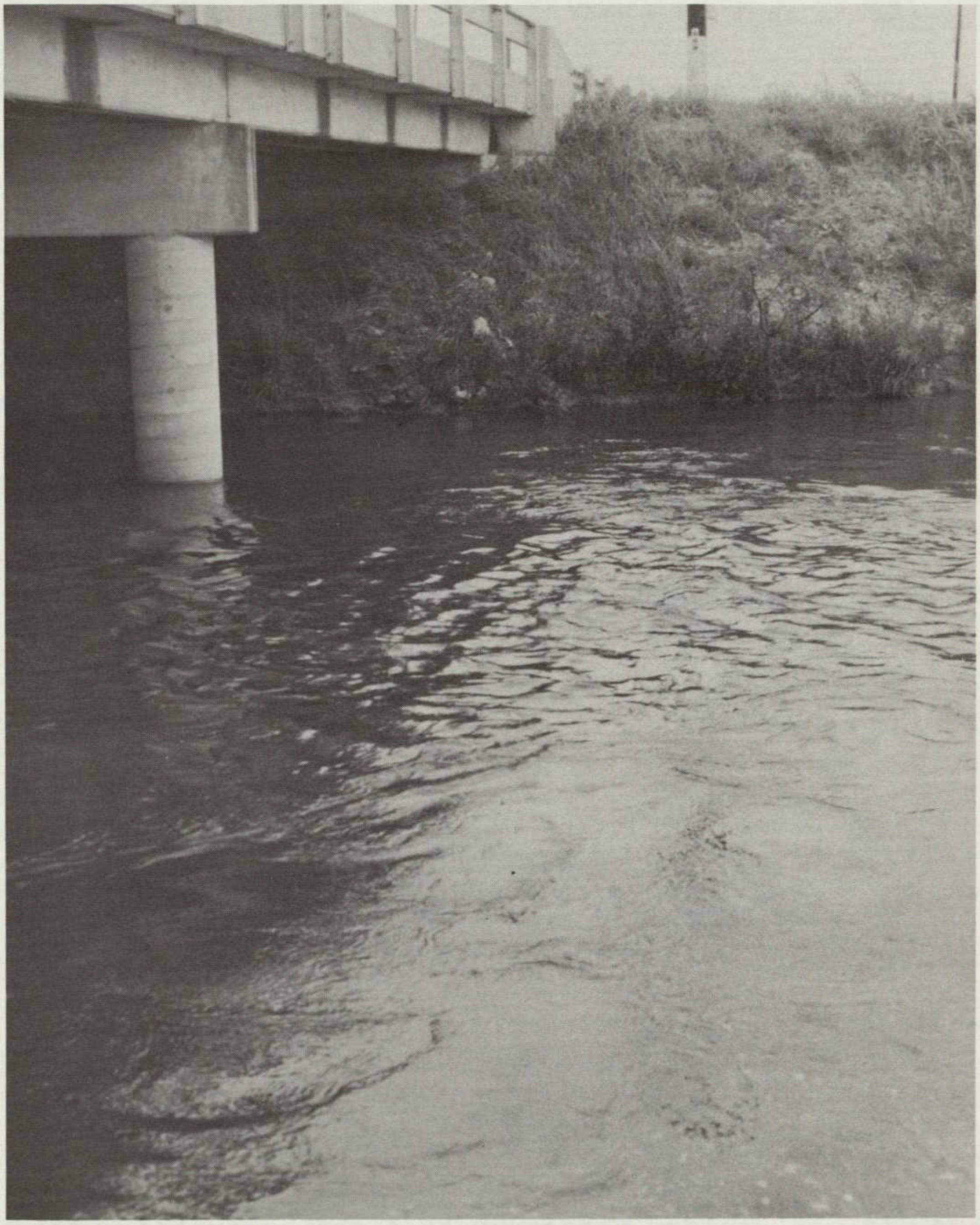

Station No. 9 is also underneath road FM-2094 as is Station No. 8.

The last ground truth station, No. 10, is located where the South Canal enters Clear Lake below another cataract. Figure 3-16 is an aerial view of this station, and also shows Clear Lake. Station No. 10 is at the bridge across the South Canal shown in the picture of Figure 3-16. Figure 3-17 is a close-up of the bridge and of a fisherman. This location and the location where the North Canal enters Clear Lake are the two most prominent fishing areas for residents of the Clear Lake area.

3.2.3 Ground truth equipment

Due to the rapid flow of the heated water in the canals, it was found during preliminary temperature soundings that only one subsurface water temperature was required at each ground sampling location. Since the water temperature dropped only about two degrees during the four miles of travel between the power plant and the lake, it was decided necessary that the subsurface water temperature measuring instrument must be accurate to one-tenth of a degree Fahrenheit.

Figure 3-16. Ground truth Station 10.

This is an aerial view looking south of ground truth Station No. 10, on the South Canal. The station is located below the cataract at the bridge, where the canal water enters Clear Lake. Clear Lake is evident across the top of the picture, and private residences may be noted bordering the warmed water area. Fishing and crabbing are very good at this location, and also near Station No. 1 where the North Canal enters Clear Lake.

Figure 3-17. Close-up view of Station No. 10.

This is a close-up view of the specific location of Station No. 10, where the South Canal water mixes with Clear Lake water. A fisherman is visible near the far end of the bridge.

The heated effluent water contains much food material for the fish, and they seem to thrive in the warm areas.

The Instrumentation Division of NASA designed, fabricated, and calibrated a thermistor and bridge circuit device for measuring the water temperature. It was mounted on an eight feet long surf rod for convenience, with the thermistor probe extending about eight feet on a flexible cable from the end of the rod. The resulting thermometer was very portable, and has a response time of about fifteen seconds. Figure 3-10 is a photograph of the instrument being used. Figure 3-19 is a schematic of the circuitry. The calibration device used was a model 2800A MYDBC Digital Quartz thermometer using a model 2850A Hewlett-Packard probe, serial 545/12, National Bureau of Standards traceable. Figure 3-18 shows the relation between temperature and the three resistance ranges of the ground truth instrument.

3.3 The Flight

The air and ground data gathering operation was conducted on June 22, 1970. The RS-14 infrared scanner was operated over the canals by NASA, who was primarily interested in verifying the capabilities of the instrument.

Figure 3-18. Properties of thermistor.

This is a plot of temperatures vs. resistance values of the ground truth instrument.

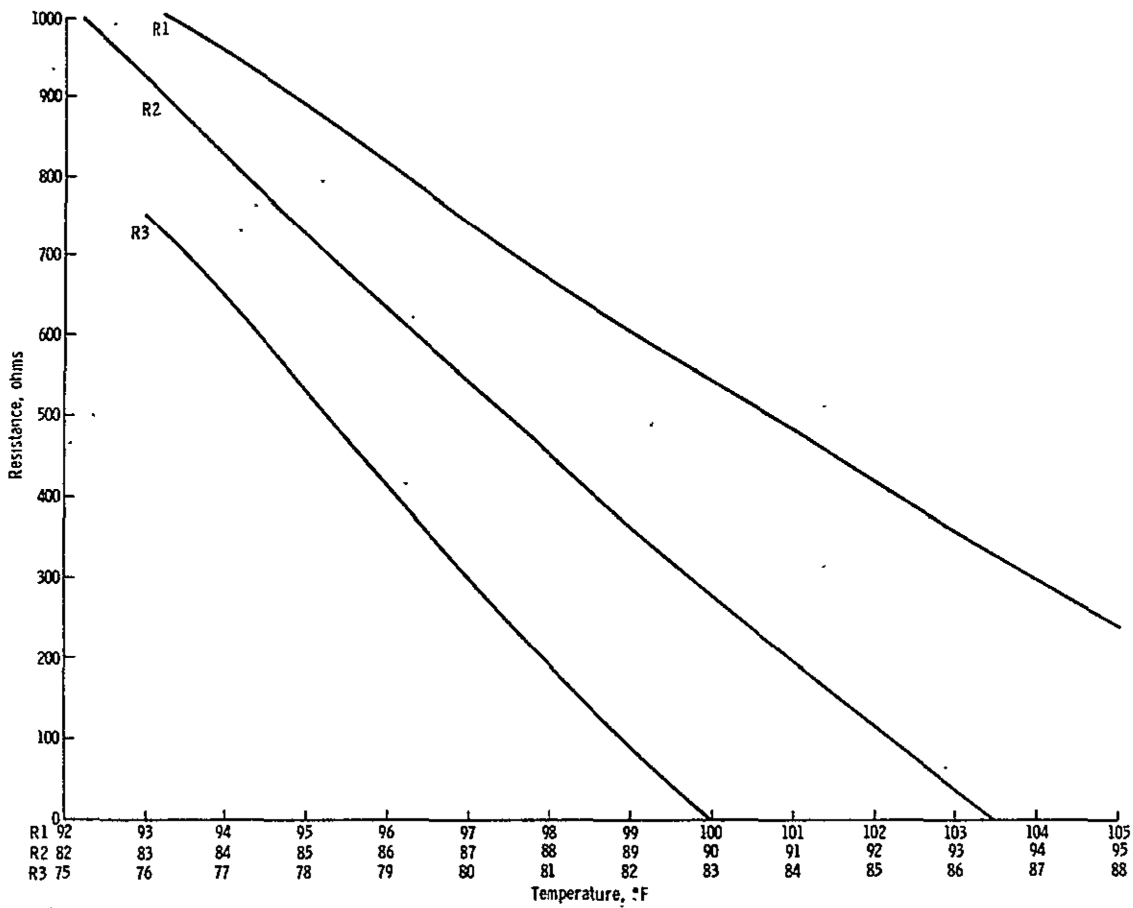

Thermister calibration

Figure 3-19. Schematic of ground truth instrument.

This is a schematic of the ground truth temperature measuring instrument.

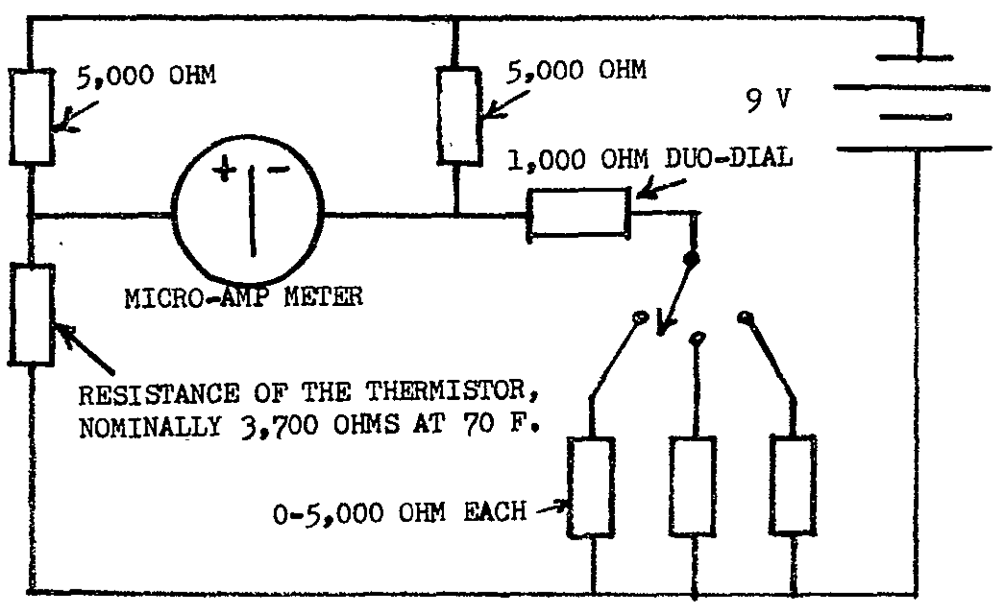
5,000 OHM
5,000 OHM
9 V
1,000 OHM DUO-DIAL
MICRO-AMP METER
RESISTANCE OF THE THERMISTOR,
NOMINALLY 3,700 OHMS AT 70 F.
0-5,000 OHM EACH

This was the first time the scanner was used to image a temperature range near 100 degrees Fahrenheit.

The aircraft crew brought the scanner to operating level while the aircraft was on the ramp at Ellington Air Force Base. A 105.12 degree Fahrenheit blackbody was placed beneath the aircraft within view of the scanner optics and the infrared radiation emitted was recorded as a temperature reference on the RS-14 film.

The scheduled take-off of the aircraft was 0900, however the actual take-off was 1004. The 0900 time was established so that the water in the canals would have a uniform temperature gradient, resulting from a somewhat uniform power load that is usual of the early morning hours. The power plant began a gradual increase in its load at 1000, and the data were expected to show an associated temperature rise of the canal water near the power plant.

Prior to the flight, the power company volunteered to maintain a constant flow through their condensers between the hours of 0900 and 1100. This was done and the flow throughout the mission was maintained at 400,000 gallons per minute.

Temperatures of the canal water were recorded in sequence beginning with Station No. 1 and ending with Station No. 10, as planned. The first measurement was at 0914 and the last at 1055.

The aircraft and scanner was over the heated effluent canals and began the first of eleven flight lines at 1034. The lines had been established to include all the ground data stations, and are shown in Figure 3-20. The lines were flown at an altitude of 1300 feet and a speed of 150 knots, which were the minimum values that would result in contiguous line scanning of the terrain below the aircraft. The RS-14 scanner compensates for roll of the aircraft up to eight degrees, and should this limit be exceeded the film data would show some distortion, so the flight lines and turns were flown with a minimum of aircraft roll. This requirement increases the turn radii and flight time. During the flight the scanner functioned properly, and five metric mapping cameras were also operated over the canals for documentary purposes.

The sky was partly cloudy and some ground haze existed just prior to the flight; however, the haze left the test area and the clouds parted to allow very

Figure 3-20. Map of flight lines.

The eleven flight lines are shown on this illustration, and their relation to the ten ground data stations.

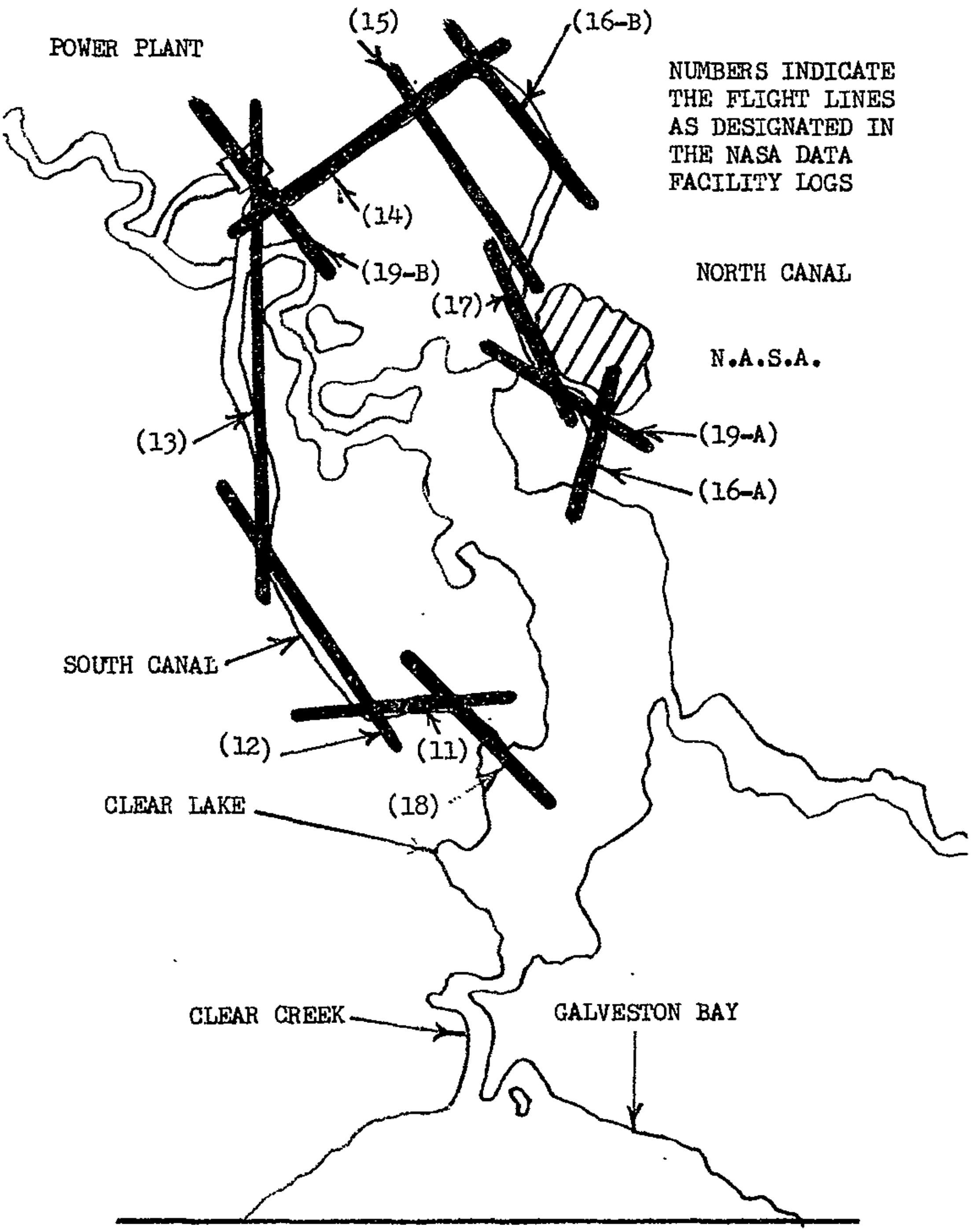
POWER PLANT
(15)
(16-B)
NUMBERS INDICATE THE FLIGHT LINES AS DESIGNATED IN THE NASA DATA FACILITY LOGS
(14)
(19-B)
NORTH CANAL
(17)
N.A.S.A.
(13)
(19-A)
(16-A)
SOUTH CANAL
(12)
(11)
(18)
CLEAR LAKE
CLEAR CREEK
GALVESTON BAY

acceptable conditions for airborne remote sensing operations. Should the take-off time have been an hour earlier as planned, the ground haze would most likely have been sufficient to greatly affect the infrared imagery. Figure 3-21 is an aerial view across the Manned Spacecraft Center, Clear Lake, and both canals, that shows the magnitude of the ground haze that existed during the overflight.

3.4 The Airborne Sensor

3.4.1 General

The total energy emitted by an object is a function of both thermodynamic temperature and emissivity and is expressed by the Stefan-Boltzmann Law:

$$W = KET$$

Where: W is the total radiant emittance, in watts per square centimeter.

K is the Stefan-Boltzmann constant, 5.673×10^{12} watts per square centimeter.

E is the dimensionless emissivity factor.

T is absolute or thermodynamic temperature in degrees Kelvin.

Figure 3-12. Aerial view of ground haze.

This aerial view across the Manned Spacecraft Center and both canals shows the magnitude of the ground haze that prevailed the morning of the overflight.

As infrared energy passes through the atmosphere, some energy is lost through atmospheric scattering and absorption. The amount lost depends on the radiation wavelength and the condition of the atmosphere. Atmospheric humidity, temperature, and pressure, as well as foreign particles in the atmosphere such as haze, smoke, water, and ice also affect infrared transmission. Infrared energy may be detected by "detectors" that are transducers that convert the energy to electrical signals which are amplified and processed to produce a presentation of the detected radiation.

3.4.2 Simplified block diagram description

A simplified block diagram of RS-14 system is shown in Figure 3-22 and the scanner optical system is shown in Figure 3-23. The transverse scanning motion of the modified Cassegrain optical system is provided by rotating a rectangular scan mirror about an axis parallel to the aircraft axis. Each side of the four-sided scan mirror is approximately 4 by 1.30 inches. The mirror is driven by a motor at 1000 rpm to generate 67 scans per second. Optionally, the scan drive system may be

Figure 3-22. Diagram of infrared scanner.

This is a block diagram of the RS-14 scanner system.

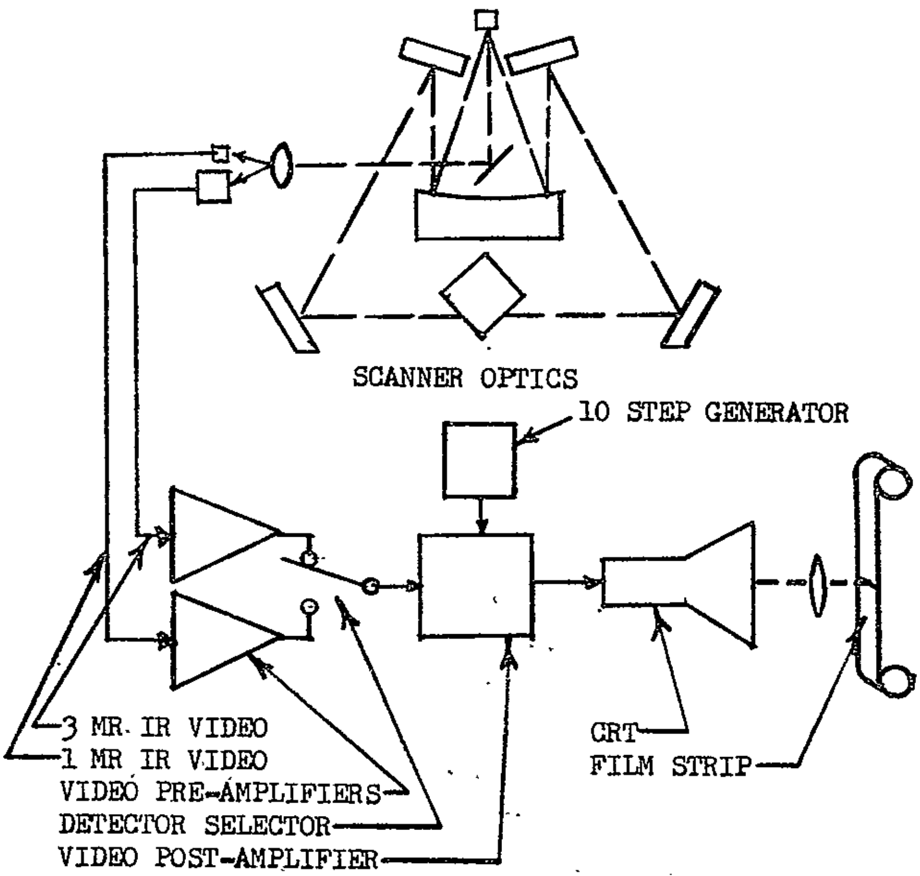
SCANNER OPTICS
10 STEP GENERATOR
3 MR IR VIDEO
1 MR IR VIDEO
VIDEO PRE-AMPLIFIERS
DETECTOR SELECTOR
VIDEO POST-AMPLIFIER
CRT
FILM STRIP

Figure 3-23. Infrared scanner optics.

This is a ray diagram of the RS-14 optics.

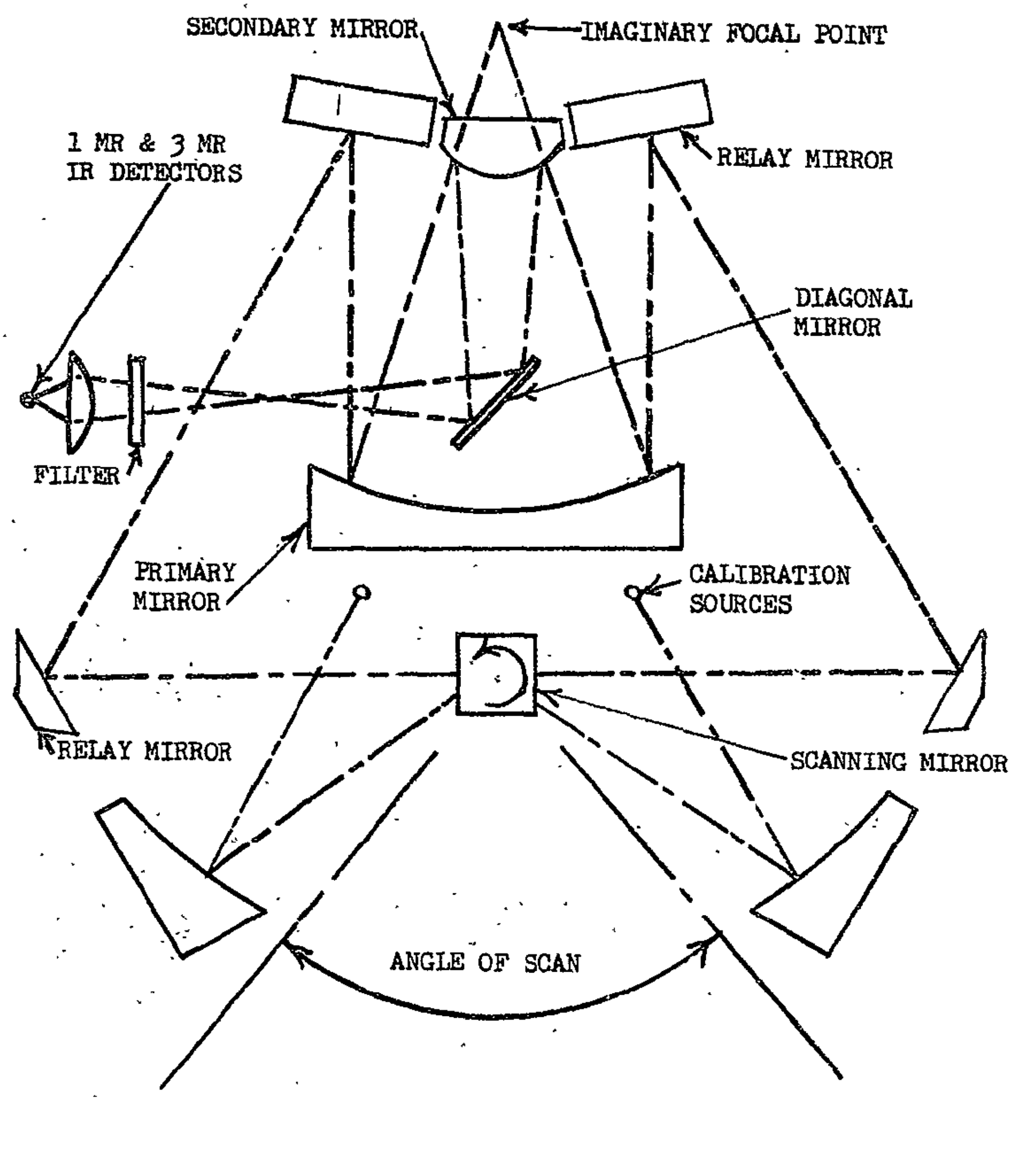
SECONDARY MIRROR
IMAGINARY FOCAL POINT
1 MR & 3 MR
IR DETECTORS
RELAY MIRROR
DIAGONAL
MIRROR
FILTER
PRIMARY
MIRROR
CALIBRATION
SOURCES
RELAY MIRROR
SCANNING MIRROR
ANGLE OF SCAN

converted to operate at 3000 rpm (200 scans per second). This rotating element scans a total field of view of 80 degrees centered about the aircraft ground track.

Flat relay mirrors reflect the radiation to the primary focusing element, an ellipsoidal mirror. This mirror, with a secondary (spherical) mirror produces a 40-inch effective focal length optical system to this point. This image now becomes a virtual object which is reimaged by the relay lens to produce an effective system focal length of 10 inches, with an unobscured collecting aperture of approximately 5.8 square inches and an optical resolution capability of 1.0 and 3.0 milliradans (MR). The secondary mirror's position is fixed and does not need to be moved (focused) for any altitudes above 500 feet.

The detectors convert incident infrared energy to acceptable electrical signals only when they are cooled to a very low temperature.

The RS-14 is a passive infrared and ultraviolet imaging system that scans the ground area along the aircraft flight path and produces a rectilinear photographic film map of the earth terrain. During this

study the ultraviolet capability of the system was not used.

The system is passive in that it detects and records variations in radiant energy emitted from earth terrain. Information received by the system is converted to video intelligence and processed through the system electronics. The video intelligence is converted to light energy and displayed to the system operator, and is recorded on photographic film in the form of a continuous strip. The video intelligence is also recorded on magnetic tape and can be reconverted to film strip if desired.

The optical system of the RS-14 gathers and focuses incoming radiation on two mercury-doped germanium detectors that are cryogenically cooled and respond to energy in the 8 and 14 micron region of the electromagnetic spectrum.

The cryogenic cooling unit maintains the detectors at 26 degrees Kelvin or less to ensure good detector sensitivity and low noise at infrared frequencies. The two germanium detectors have different size apertures in order to provide flexibility in the selection of

maximum spatial resolution or maximum thermal resolution of the incoming energy as recorded on the airborne film.

The electrical signal from the detector selected for use is processed and supplied to a magnetic tape recorder. The signal is displayed as an intensity-modulated trace on a five-inch cathode-ray tube in the film recorder unit and exposes a strip of film whose travel is controlled by the ratio of aircraft velocity to aircraft height as established by the system operator on the control panel. The RS-14 compensates for aircraft roll, and the film shows a high-resolution rectilinear map of the infrared characteristics of the mapped terrain. This condition is provided by a cryogenic refrigerator or cooler in which the detectors are mounted. The detectors are single crystal, extrinsic, photoconductive devices that are composed of mercury-doped germanium. They are bulk absorbers of energy ranging from 8 to 14 microns in wavelength. A metal box with a small aperture (cold shield) surrounds the useful field of view. The sensitive areas of the detectors are located near the focal point of the scanner optic system. The relay lenses previously mentioned are used in place of

a cooler "window" to seal off the cooler's vacuum jacket from the atmosphere.

3.4.3 Technical characteristics

The RS-14 was manufactured by the Texas Instruments Company for NASA to the following specifications:

Characteristic	Specification
Ambient Temperature Limitations	-54 to +55 Centigrade
Altitude Limitations	50,000 feet
Input Power Requirements	
AC voltage	115 VAC, e phase, 400 Hertz
AC power	3200 va
DC voltage	28 vdc
Lateral Scan Angle	40 degrees either side of nadir
Scan Rate	66.7 per second (3 mil) 200 per second (1 mil)
Instantaneous Field of View	1 milliradian 3 milliradian
Noise Equivalent Temp. (NET)	Less than 0.5 C for 1MR Less than 0.3 C for 3MR
Velocity to Height Ratio	0.02 to 0.2 radians/sec
Detectors	Mercury-doped germanium at 1MR and 3MR
Detector cooling	Closed cycle helium, 24K

Stabilization	Roll + 8 degrees
Recording Format	2.8 inches of Video, 1 inch Auxiliary data
Recording Film	350 feet; 5 inches wide, S)-2498
Bandwidth	1MR = 315 K Hz 3MR = 35 K Hz
Angular Resolution	1MR and 3MR

CHAPTER IV

RESULTS

4.1 Summary

The MSC photographic laboratory processed the film exposed during the flight on June 22. The negatives were reviewed by the aircraft instrument operator and engineers, and were considered acceptable. The RS-14 and camera systems had operated within design limits during the overflights.

Visual observation of the RS-14 imagery of the canal water showed that approximately four levels-of-gray were evident between the hot water emerging from the power plant at Station No. 6, and the heated canal water as it left the canals and entered Clear Lake at Stations No. 10. By visually comparing the contrast levels of the canal waters with any two known ground water temperatures, a quick temperature quantity could be established for any location along the canals.

Four KA-62 multiband cameras having image motion compensation and using panchromatic film and an RC-8

metric camera using color-shifted infrared film had been used during the flight, and the film from each camera had also exposed properly.

The transparent copies of the RS-14 film had slightly more contrast than the original film, therefore it was decided that the original flight negative would be used for obtaining isodensity tracings of the ground truth station locations. These tracings would be representative of water temperature as extrapolated from a straight line function between the high temperature preflight calibration source and the instrument housing temperature, both as imaged on the film along with the ground scene. Positive prints of the camera negatives, and of the RS-14 original negatives, were representative of the flight negatives, and were used in this report for documentation purposes.

Appendix A contains prints of the RS-14 data as obtained during each flight line. Appendix B contains black and white infrared and Appendix C contains color infrared photographs of the ground data stations as recorded during the data runs of the scanner. The thermal imagery is described within this chapter.

4.2 Ground Truth

Table 4-1 is a listing of the ground truth temperature data recorded during the overflight of the RS-14. The data shows the ground truth station number, the local time that the temperature was recorded, the highest and lowest readings on the thermistor resistor, the resistor scale, and the temperature of the water at that station.

The flow through the power plant was maintained at 400,000 gallons per minute during the experiment. The canals have side slopes of 2:1 and flat bottoms to minimize erosion of the banks. The North Canal is 40 feet wide at the water level during maximum flow, and the South Canal is 70 feet wide. To maintain equal and minimum water velocities in the two canals, flow in each canal is considered to be proportional to cross-sectional areas of each canal. The North Canal has 150 square feet of cross-section and the South Canal has 300 square feet, therefore for this study one-third, or 133,000 gallons per minute are considered to flow in the North Canal and 266,000 in the South Canal.

The heat liberated to the water as it flows through

TABLE 4-1

GROUND TRUTH DATA

Station Location	Time Zulu	Thermistor High	Thermistor Low	Scale	Temperature Fahrenheit
1	1412	080	076	2	92.5
2	1421	058	056	2	92.8
3	1342	962	958	1	93.9
4	1439	896	891	1	94.8
5	1444	874	868	1	95.2
6	1500	560	555	1	99.8
7	1510	712	710	2	85.2
8	1543	060	058	2	92.7
9	1549	055	047	2	92.9
10	1555	940	935	1	94.2

This table shows the subsurface water temperature at each of the ground data stations.

the condensers of the power plant varies with the electrical load being generated, therefore it is possible for canal water downstream from the plant to be warmer than canal water nearer to the plant. During this study water temperature measurements were recorded at discrete locations along the canals and straight-line temperature gradients were assumed between the ground stations. Heat liberated from the water between the ground stations was calculated using the steady-state relations:

$$\text{Heat Lost} = (W)\ (C)\ (Ta\text{-}Tb)$$

Where: W = water flow in pounds per unit time

C = specific heat of water

Ta-Tb = temperature difference between stations

As a typical calculation, the heat lost from the canal water, using ground data, between stations No. 1 and 2 was

$$\begin{aligned}\text{Heat Lost} &= (W)\ (C)\ (Ta\text{-}Tb)\\ &= (133{,}000)\ (8.33)\ (1)\ (92.8\text{-}92.5)\\ &= 334{,}000 \text{ BTU's per minute}\end{aligned}$$

Although a detailed thermal energy balance of these canals would involve more study and calculations, this approximation was considered adequate for the purpose of this research. Table 4-2 shows the results of these heat calculations between each data station along the canals, as obtained using ground water temperatures.

4.2 Airborne Data

Three methods were used to extract temperatures from the RS-14 data film, described as follows:

4.3.1 Method 1: Photointerpretation of the film

Along the edge of the imaged scene the RS-14 produces a 10-step density strip, each step one inch in length and one-fourth inch wide. This step-wedge is produced completely independent of any operator settings or signal intensity from the ground, and is repeated continuously throughout the length of the film. The 10-step wedge is visible on the prints of the RS-14 data film in this report. This wedge serves as a visual reference for gray levels.

The calibration blackbody that was held within view

TABLE 4-2

HEAT EXCHANGE USING GROUND DATA

Between Stations	Ta Fahrenheit	Tb	Heat Liberated BTU's per Min.
1-2	92.8	92.5	+ 332,400
2-3	93.9	92.8	+ 1,218,800
3-4	94.8	93.9	+ 997,200
4-5	95.2	94.8	+ 443,200
5-6	99.8	95.2	+ 5,096,800
6-8	99.8	92.7	+14,733,600
8-9	92.7	92.9	- 443,200
9-10	92.9	94.2	- 2,880,800

This table shows heat flow from the canal water between the ground stations, using subsurface temperatures as recorded in the canal water during the overflight.

of the scanner optics prior to the flight produced an image approximately one-half inch wide on the RS-14 data film, shown in Figure 4-1, representing a gray level of 103.55 degrees Fahrenheit. When the data film is viewed over a lighted table, the film density produced by this blackbody visually corresponds to the density of step-wedge number 10, therefore gray levels in the imaged scene corresponding to step-wedge 10 were considered to be 103.55 Fahrenheit or higher. Since the canal water could not feasibly be higher than 105 degrees Fahrenheit, this gray level established an upper limit for photo-interpreting temperatures from the data film.

Along one edge of the RS-14 data film there is also a continuous strip approximately one-fourth inch wide that is a density recording of the scanner housing temperature. This housing is a heavy casting having a unity-emissivity coating, and having a thermistor mounted within the area viewed during each scan of the RS-14 mirror. The temperature of this thermistor is recorded by the operator at the beginning and end of each flight line. Once at a given altitude the scanner

Figure 4-1. Preflight calibration image.

This is a picture of the RS-14 data film showing the thermal image of the preflight calibration black-body.

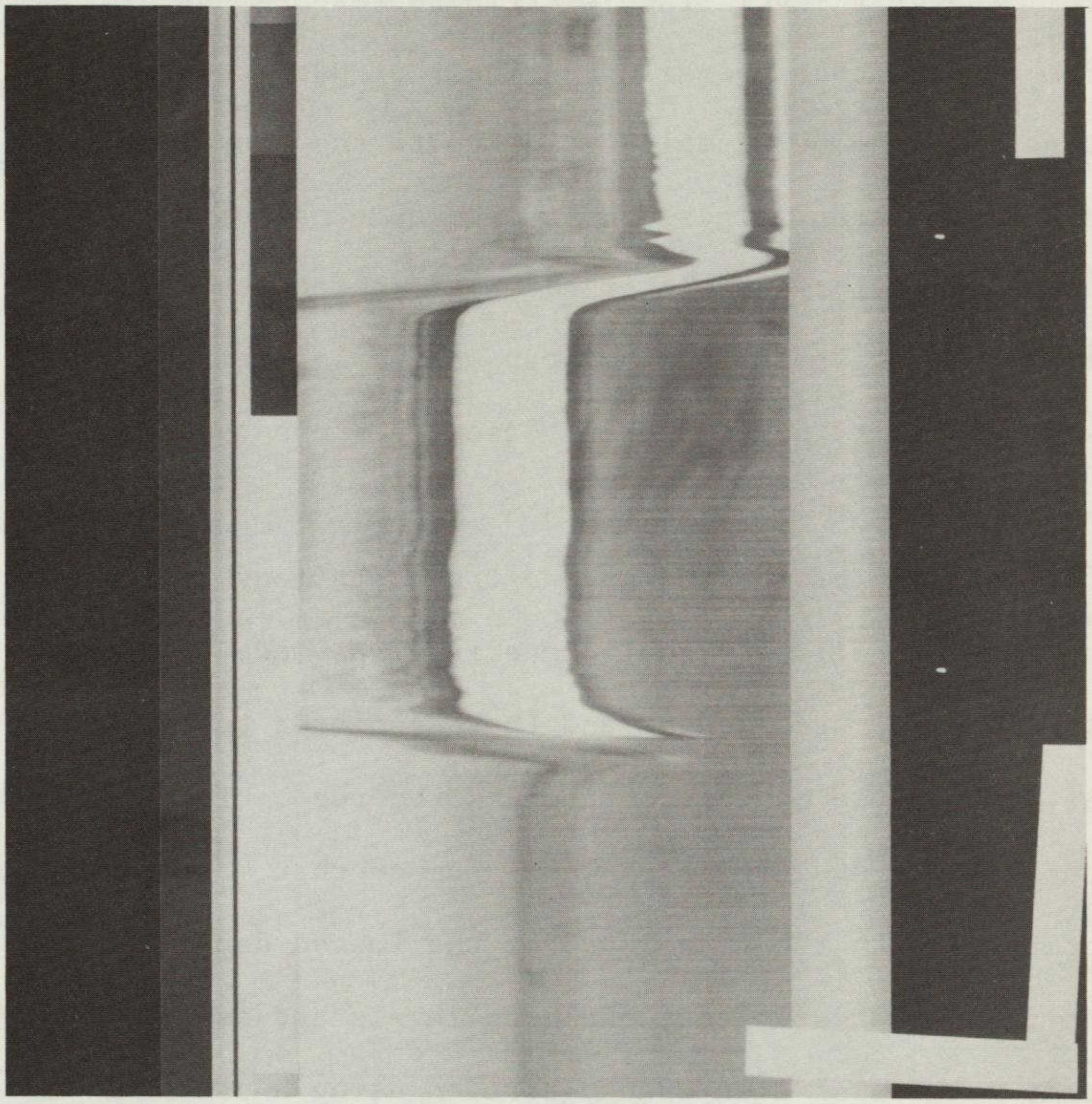

housing temperature quickly stabilizes and appears to maintain a near-constant value.

The gray level of this strip represents the housing temperature that prevailed during that particular flight line, and can be visually compared to the gray level of one of the step wedges. This procedure establishes a lower limit for photointerpreting temperatures directly from the data film and the step wedges between the high and low limits can represent discrete ground apparent temperatures.

At each of the ten ground truth stations as imaged on the data film a visual comparison was made to a gray level on the step-wedge, and the associated temperature as interpreted by this method was recorded. Table 4-3 shows the gray-level step-wedge number that most nearly compares with the gray level of the imaged canal water at the ground stations, the step levels and associated temperatures of each ground station using a straight line relation between the two calibration temperatures.

TABLE 4-3

METHOD 1: PHOTOINTERPRETATION OF THE FILM

Station	Flight Line	Step Wedge	Housing Step	Housing Temp.	Pre-Cal. Step	Pre-Cal. Temp.	Station Temp.
1	16-A	3.5	7	96.8	10	103.55	89.0
2	16-A	2.5	7	96.8	10	103.55	86.8
3	17	3.0	7	96.35	10	103.55	86.8
4	16-B	5.0	7	96.8	10	103.55	92.4
5	14	5.5	7	95.9	10	103.55	92.2
6	19-B	5.5	6.5	97.25	10	103.55	95.4
7	19-B	1.5	7	97.25	10	103.55	85.8
8	13	4.0	7	95.0	10	103.55	86.4
9	11	3.5	5.5	94.55	10	103.55	90.7
10	18	3.5	7	96.8	10	103.55	89.0

This table shows the ground station water temperature using Method 1, as depicted by comparing step-wedge gray levels with both the imaged canal water and the imaged calibration sources. The low calibration gray level and temperature was the imaged scanner housing, and the high calibration source was the blackbody imaged preflight.

4.3.2 Method 2: Photointerpretation using ground truth

The second method used was to select a warm and a cool ground station temperature, and visually compare the gray level images of these two temperatures with the ten-step. Again, a straight-line division of temperatures as represented by the ten-step wedge was established, and the temperatures of the remaining eight ground stations were interpreted from visual comparisons of the gray levels as recorded on the RS-14 data film. The image of the inlet water at Station No. 7 was used as the cool gray level and the water at Station No. 6 was used as the warm gray level. Table 4-4 shows the ground station water temperatures using this method.

4.3.3 Method 3: Machine use

The third method was to use a microdensitometer to analyze the RS-14 film densities. The instrument was calibrated to divide levels of gray into eight distinct steps. The most dense of these represented the temperature of the 105.12 degrees Fahrenheit internal calibration course and the lest dense represented 89 degrees

TABLE 4-4

METHOD 2: PHOTOINTERPRETATION USING GROUND TRUTH

Station	Flight Line	Step Wedge	Ground Lo-Cal Step	Ground Lo-Cal Temp	Ground Hi-Cal Step	Ground Hi-Cal Temp	Station Temp
1	16-A	3.5	1.5	85.2	5.5	99.8	92.6
2	16-A	2.5	1.5	85.2	5.5	99.8	89.0
3	17	3.0	1.5	85.2	5.5	99.8	90.9
4	16-B	5.0	1.5	85.2	5.5	99.8	98.0
5	14	5.5	1.5	85.2	5.5	99.8	99.8
6	19-B	5.5	1.5	85.2	5.5	99.8	99.8
7	19-B	1.5	1.5	85.2	5.5	99.8	85.2
8	13	4.0	1.5	85.2	5.5	99.8	94.4
9	11	3.5	1.5	85.2	5.5	99.8	92.6
10	18	3.5	1.5	85.2	5.5	99.8	92.6

This table shows the canal water temperatures as established using Method 2. The temperatures were determined using a straight line function of the gray levels imaged from two known ground water locations.

Fahrenheit. The two reference points used were the gray level images of the internal calibration blackbody and the RS-14 housing.

Isodensity tracings of the water at each ground station as imaged on the RS-14 data film were made, and the predominant temperature of the water at this station was recorded. These tracings were made with a 10 micron spot width, and a magnification of 10 times the originally imaged ground station scene. The tracing lines were spaced 500 microns apart.

Figure 4-2 is an isodensity tracing of Station No. 9, and a schematic of the tracing showing the specific location where the temperatures were recorded in the canal water. This figure is shown as being typical of all the tracings. Figure 4-3 is a print of the thermal imagery as recorded of Station No. 9. Ground truth measurements of Station No. 9 established the actual subsurface water temperature as 92.9° Fahrenheit, whereas the isodensity tracing established the radiometric temperature of the station at 92° Fahrenheit. These temperatures are shown in Table 4-5.

Figure 4-2. Isodensity of Station No. 9.

This is an isodensity tracing of Station No. 9 and a graphic representation of the imaged scene. The tracing is magnified ten times the actual RS-14 image.

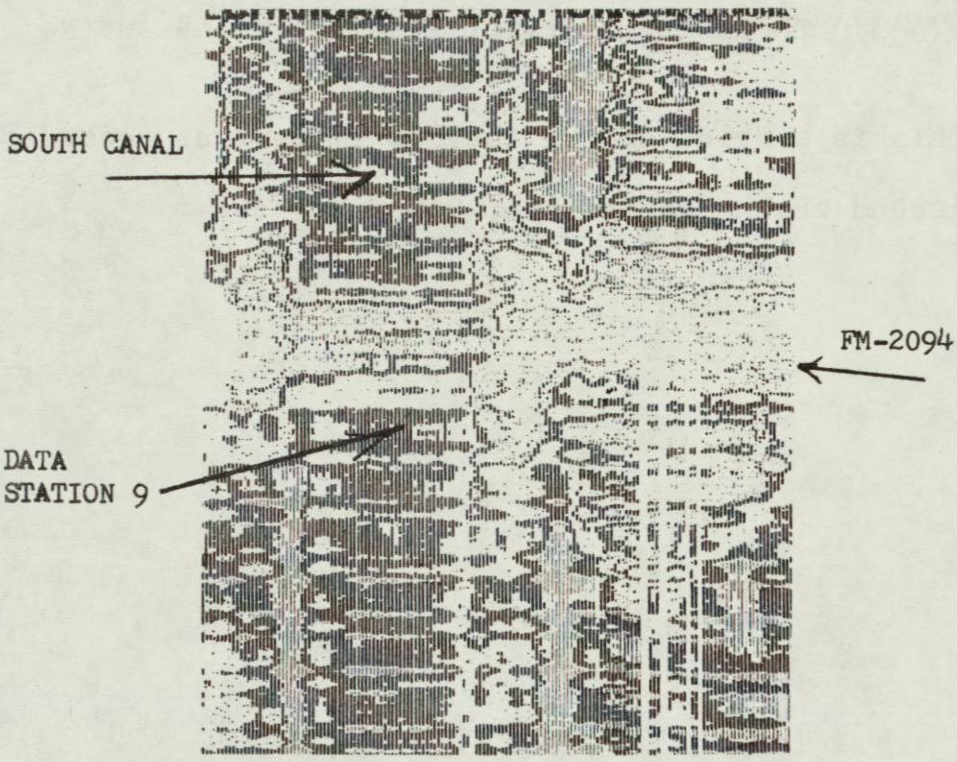
SOUTH CANAL
FM-2094
DATA
STATION 9

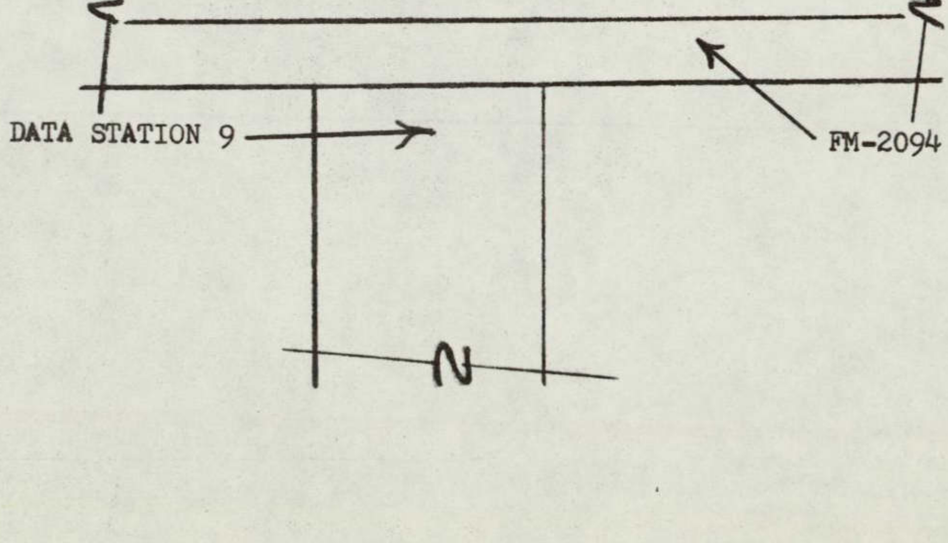
SOUTH CANAL
DATA STATION 9
FM-2094

Figure 4-3. Thermal imagery of Stations No. 9 and No. 10.

This is a print of the thermal imagery as recorded over ground truth Stations No. 9 and No. 10.

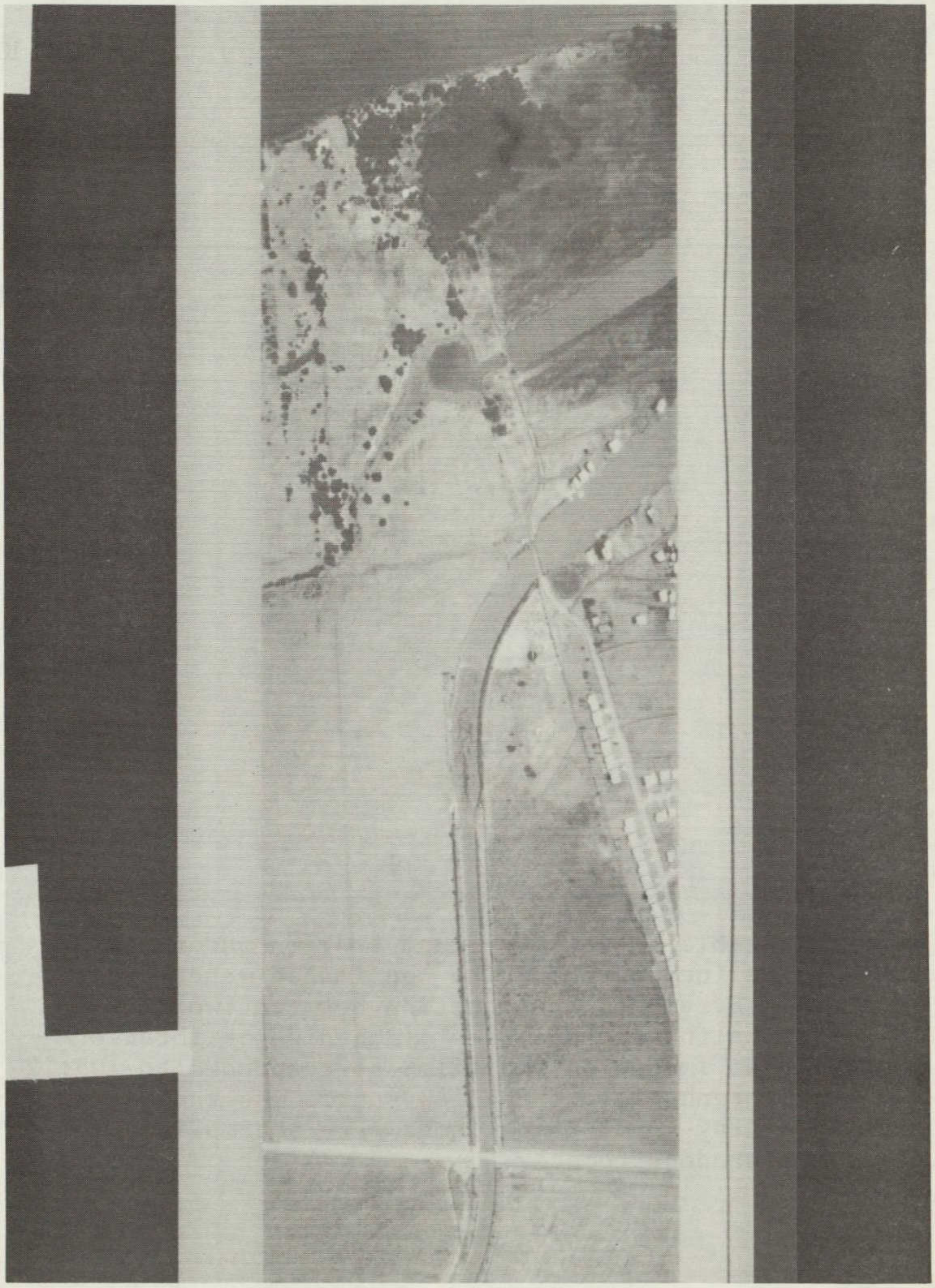

TABLE 4-5

METHOD 3: MACHINE USE

Station	Flight Line	Station Temp
1	16-A	92
2	16-A	94
3	17	95
4	16-B	94
5	14	94
6	19-B	98
7	19-B	87
8	13	94
9	11	92
10	18	94

This table shows the ground station water temperatures as defined by comparing the imaged water gray-level to a straight line function between two gray levels of calibration sources. The high calibration source, also imaged on the film, corresponded to 105.12 degrees Fahrenheit, and the low source was the scanner housing. Gray-level comparisons were accomplished using a microdensitometer.

The machine used to determine the ground station temperatures was a Double-Beam Recording Microdensitometer, Mark III C9, Serial 1014, mady by Joyce, Loebl and Company, Limited, Electron House, Princeway, Team Valley Gateshead-on-the Tyne II, England. The electronics were a Tech/OPS Isodonisitracer model 608, Serial 17.

4.4 Evaluation

Temperatures of coolant water effluent from a power plant have been derived using three methods of interpreting aerial 8-14 micron thermal imagery. These temperatures are shown in Table 4-6, along with the subsurface temperatures of the effluent as recorded on the ground. Table 4-7 shows the errors in percent between the photointerpreted water temperatures and the measured subsurface temperatures. It is evident from these values that even gross interpretation of thermal imagery can depict water temperatures within about five percent, and the more refined interpretation methods within about two-and-a-half percent.

Specific quantities are not defined in the open

TABLE 4-6

COMPARISON OF TEMPERATURES

Station	Ground Method	Method 1	Method 2	Method 3
1	92.5	89.0	92.6	92
2	92.8	86.8	89.0	94
3	93.9	86.8	90.9	95
4	94.8	92.4	98.0	94
5	95.2	92.2	99.8	94
6	99.8	95.4	99.8	98
7	85.2	85.8	85.2	87
8	92.7	86.4	94.4	94
9	92.9	90.7	92.6	92
10	94.2	89.0	92.6	94

This table shows the subsurface water temperatures measured on the ground and the interpreted station temperatures using each of the three photographic methods.

TABLE 4-7

TEMPERATURE ERRORS FROM GROUND MEASUREMENTS (%)

Station	Method 1	Method 2	Method 3
1	-3.78	+0.11	-0.54
2	-6.46	-4.10	+1.29
3	-7.57	-3.20	+1.17
4	-2.53	+3.38	-0.84
5	-3.15	+4.84	-1.26
6	-4.41	0.00	-1.81
7	+0.70	0.00	+2.11
8	-6.79	+1.83	+1.40
9	-2.37	-0.32	-0.97
10	-5.52	-1.70	-0.21
Averages	4.23%	2.44%	1.16%

This table shows the errors, in percent, between the measured ground temperatures and the interpreted temperatures.

literature of thermal mapping temperature accuracies desired for synoptic aerial subsurface temperature measurements, however the amount of error encountered here is comparable to that involved in measuring water current flown and compositions. Results of remote temperature measuring using methods one and two may be obtained quickly without the aid of digital data reduction techniques, and it appears that the associated errors would be tolerated by the ecologist concerned with monitoring gross changes in mixing zones.

Table 4-8 shows the calculated steady-state heat values that would be exchanged between the water and atmosphere should the canals be considered as constant flowing thermal conductors insulated on all sides except the top water surface. These heat values are directly proportional to the station temperatures. Although the interpreted station temperatures from the airborne methods are close to the measured subsurface temperatures, the differences are additive when calculating heat flow. This table shows errors of 26 percent between using gross photointerpreted temperatures

TABLE 4-8

CALCULATED HEAT (BTU's PER MINUTE)

Between Stations	Ground Method	Method 1	Method 2	Method 3
1-2	+ 332,400	- 2,326,800	- 3,988,800	+ 2,216,000
2-3	+ 1,218,800	0	+ 2,105,200	+ 1,108,000
3-4	+ 997,200	+ 6,204,800	+ 7,866,800	- 1,108,000
4-5	+ 443,200	- 221,600	+ 1,994,400	0
5-6	+ 5,096,800	+ 3,545,600	0	+ 4,432,000
6-8	+ 14,733,600	+ 19,914,000	+ 11,966,400	+ 8,864,000
8-9	- 443,200	- 9,528,800	+ 3,988,800	+ 4,432,000
9-10	- 2,880,800	+ 3,767,200	0	- 4,432,000
Net Lost	+ 19,498,000	+ 14,354,400	+ 23,932,800	+ 15,512,000
Errors from Ground Measurements		-26%	+23%	-20%

This table shows the calculated heat flow between the canal water and the atmosphere, assuming steady-state conditions, and the errors that can accumulate.

and ground measurements, and of 20 percent between using machine-interpreted temperatures and ground measurements.

CHAPTER V

CONCLUSIONS

5.1 Summary

The open literature records very few cases of calibrated thermal imagery being applied directly to yield better understanding of thermal effect in natural water bodies. There appears to be a reluctance on the part of some ecologists to rely upon the unnatural appearance of line-scanned imagery, however there are numerous cases where the ecologist has relied upon natural-appearing photography of secondary effects.

Thermal imagery is not as abundant as photography, but it does display the thermal situation. The experiment herein was a first step toward showing direct application of high-altitude 8-14 micron imagery, and was designed to display the realism that does exist between thermal imagery gray levels and temperatures existing in imaged water.

5.2 Recommendations

The next logical step toward delineation of thermal mixing boundaries by remote-sensed thermal imagery seems to be the conducting of an experiment in a large natural bay where a direct correlation is established between the subsurface temperature pattern and the water surface as imaged from a reasonable altitude. The thermal imagery in Appendix A of flight lines 11 and 16-A show thermal mixing zones in Clear Lake. Whether the subsurface mixing zones were at the locations imaged by the scanner is not known, however.

Galveston Bay appears to be an ideal location for conducting such a study. This bay is similar to other southern bays in physical characteristics, water ecology, and relation to the economy. Water movement in and out of the bay is not violent and subsurface mixing zones should be somewhat stable. Such an experiment should help greatly to establish direct quantitative applications of 8-14 micron thermal imagery to water ecology studies.

BIBLIOGRAPHY

1. John R. Clark, "Heat Pollution," Nat. Parks, Vol. 42, pp. 4-8, December 1969.

2. Robert H. Boyle, "The Nukes Are in Hot Water," Sports Illus., Vol. 30, pp. 24-28, January 20, 1969.

3. A. Wolff, "America's Environmental Problems," Look, Vol. 33, pp. 28-33, November 4, 1969.

4. L. Bajorunas, "Thermal Pollution: A Threat to the Cayuga's Waters," Science, Vol. 163, pp. 517-518, February 7, 1969.

5. John R. Clark, "Thermal Pollution and Aquatic Life," Sc. Am., Vol. 220, pp. 18-27 and 148, March 1969.

6. John Cairns, Jr., "Heating Up Lake Cayuga," Sci. and Cit., Vol. 10, pp. 141, June 1968.

7. Edward Muskie, "Atom Power Plant in Hot Water," Bsns. Wk., pp. 69-70, June 29, 1968.

8. Editorial, "Cayuga's Waters: Thermal Pollution by a Proposed Power Plant," Nation, Vol. 207, pp. 709, December 30, 1968.

9. J. Cairns, Jr., "We're in Hot Water," Sci. and Cit., Vol. 10, pp. 187-195, October 1968.

10. Editorial, "Scientist Questions Reactor Effects," Sci. and Cit., Vol. 10:187, pp. 154-149, August 1968.

11. Jack B. Pearce, "Thermal Addition to the Marine Environment," Science, Vol. 157, pp. 1080, September 1, 1967.

12. John Lear, "The Crisis in Water: Its Sources, Pollution, and Depletion," Sat. R., Vol. 48, pp. 23-28, pp. 78-80, October 23, 1965.

13. Editorial, "Presidential Findings on Air, Water Pollution," Am. City, Vol. 80, pp. 8, December 1965.

14. Editorial, "Federal Water-Pollution Control Act Uses Both Carrot and Stick," Am. City, Vol. 80, pp. 17, December 1965.

15. John J. A. McLaughlin, "Aquatic Pollution," Science, Vol. 146, pp. 281-288, October 9, 1964.

16. Luther L. Terry, "Pollution of U.S. Air and Water--How Serious?" U.S. News, Vol. 55, pp. 98-105, September 16, 1963.

17. Editorial, "Sitting on a Volcano," Am. For., Vol. 70, pp. 11, September 1964.

18. National Conference on Water Pollution, "Thirteen Steps to Cleaner Surface Water," Am. City, Vol. 76, pp. 32, February 1961.

19. Carl H. Strandberg, "Water Quality Analysis," Photo. Eng., Vol. 32, pp. 234-248, March 1966.

20. Peter C. Badgley, "Planetary Exploration from Orbital Altitudes," Photo. Eng., Vol. 32, pp. 250-259, March 1966.

21. Eugene E. Derenyi and Gottfried Konecny, "Infrared Scan Geometry," Photo. Eng., Vol. 32, September 1966.

22. Peter C. Badgley, "Orbital Remote Sensing and Natural Resources," Photo. Eng., Vol. 32, pp. 780-790, September 1966.

23. James H. McLerran, "Infrared Thermal Sensing," Photo. Eng., Vol. 33, pp. 507-512, May 1967.

24. Richard Blythe and Ellen Kurath, "Infrared and Water Vapor," Photo. Eng., Vol. 33, pp. 772-777, July 1967.

25. Jack R. VanLopik, Albert E. Pressman, and Roger L. Ludlum, "Mapping Pollution with Infrared," Photo. Eng., Vol. 34, pp. 561-564, June 1968.

26. Edward F. Yost and Sondra Wenderoth, "Multispectral Color Aerial Photography," Photo. Eng., Vol. 33, pp. 1020-1033, September 1967.

27. Earl S. Leonardo, "Capabilities and Limitations of Remote Sensors," Photo. Eng., Vol. 30, pp. 1005-1010, November 1964.

28. David E. Harris and Caspar L. Woodbridge, "Terrain Mapping by Use of Infrared Radiation," Photo. Eng., Vol. 30, pp. 134-139, January 1964.

29. Carl H. Strandberg, "Analysis of Thermal Pollution from the Air," Photo. Eng., Vol. 29, pp. 656-671, July 1963.

30. L. Eugene Cronin and David A. Flemer, "Energy Transfer and Pollution," Natural Resources Institute of the University of Maryland, Chesapeake Biological Laboratory, Solomons, Maryland, Interstate Publishers 1967.

31. L. Eugene Cronin, "Patuxent Thermal Studies," Chesapeake Biological Laboratory Natural Resources Institute, University of Maryland, January 1969.

32. L. Eugene Cronin, "The Impact of Thermal Releases Along the East Coast on Shellfish," Natural Resources Institute, University of Maryland, 1969.

33. S. Markowski, "The Cooling Water of Power Stations: A New Factor in the Environment of Marine and Fresh Water Invertebrates," Central Electricity Generating Board Biological Laboratory, London, England, 1969.

34. Mahlon G. Kelly, "Applications of Remote Photography to the Study of Coastal Ecology in Biscayne Bay, Florida," Department of Biology, University of Miami, Coral Galves, Florida, July 1969.

35. D. R. Woodward, "Availability of Water in the U.S. with Special Reference to Industrial Needs by 1980," Photo. Eng., Washington, D.C., 1957.

36. "Steam-Electric Plant Construction Cost and Annual Production Expenses"--Thirteenth Annual Supplement, 1960. Federal Power Commission.

37. Verbal communication, Carl H. Strandberg with Dr. Richard H. Strain, Strong Memorial Hospital, Rochester, New York.

38. Proceedings--"Conference on Physiological Aspects of Water Quality," U.S. Public Health Service, Washington, D.C., September 8-9, 1960.

39. Richard D. Hoak, "The Thermal Pollution Problem," Journal of the Water Pollution Control Federation, December 1961.

40. Verbal communication, Carl H. Strandberg with R. G. Godfrey, U.S.G.S., Director of Project 3254, "Dispersion in Natural Streams."

41. Milton C. Kolipinski and Aaron L. Higer, "Remote Sensing Applications to Hydrobiology," NASA Earth Resources Aircraft Program Status Review, Vol. 3, pp. 23-1/23-44, September 16-18, 1968.

42. Richard W. Paulson, "Estuarine Studies," NASA Earth Resources Aircraft Program Status Review, Vol. 3, pp. 24-1/24-10, September 16-18, 1968.

43. Este F. Hollyday, "Use of Infrared Imagery to Locate Surficial Aquifers," NASA Earth Resources Aircraft Program Status Review, Vol. 3, pp. 25-1/25-14, September 16-18, 1968.

44. Richard R. Anderson, "Remote Sensing of Marshlands and Estuaries Using Color Infrared Photography," NASA Earth Resources Aircraft Program Status Review, Vol. 3, pp. 26-1/26-23, September 16-18, 1968.

45. F. C. Polcyn, "Surface Effects and Submerged Features," NASA Earth Resources Aircraft Program Status Review, Vol. 3, pp. 46B-1/46B-18, September 16-18, 1968.

46. D. S. Lowe, "Infrared Studies," NASA Earth Resources Aircraft Program Status Review, Vol. 3, pp. 51-1/51-17, September 16-18, 1968.

47. Joel Alan Snow, "Guide to Educated Guessing," Sci. and Cit., Vol. 10:187, pp. 157-159, August 1968.

48. Daniel Merriman, "The Calefaction of a River," Sci. Am., pp. 42-52, May 1970.

APPENDIX A

THERMAL IMAGERY OF THE FLIGHT LINES

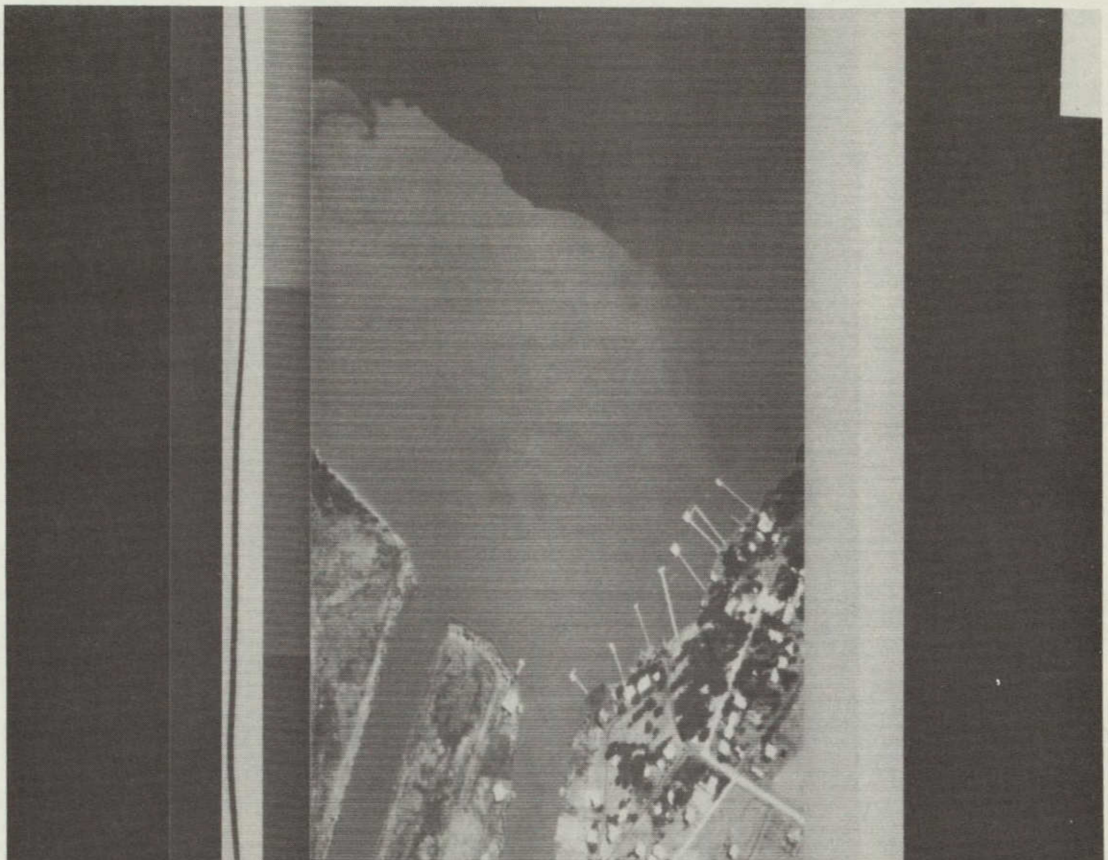

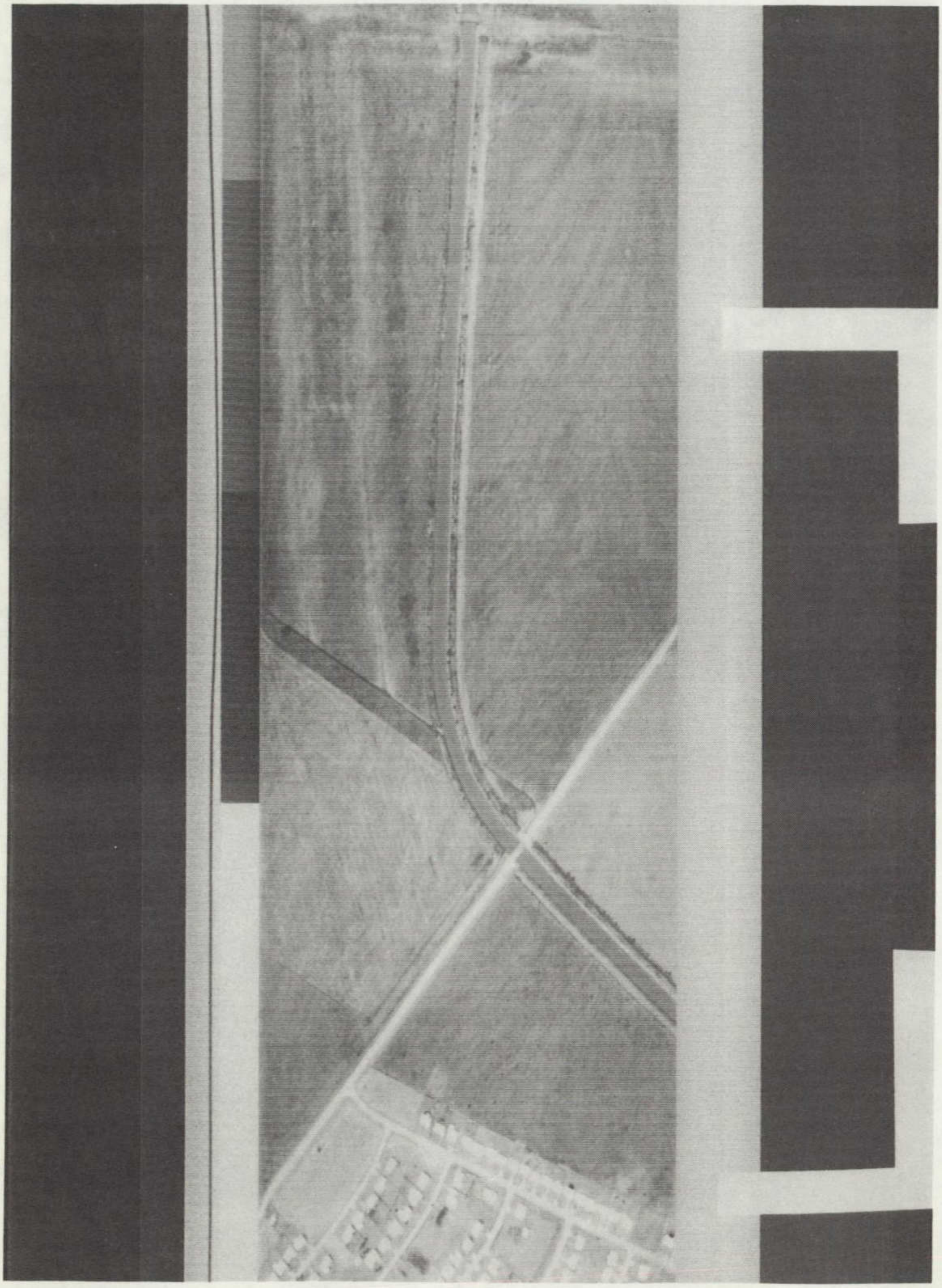

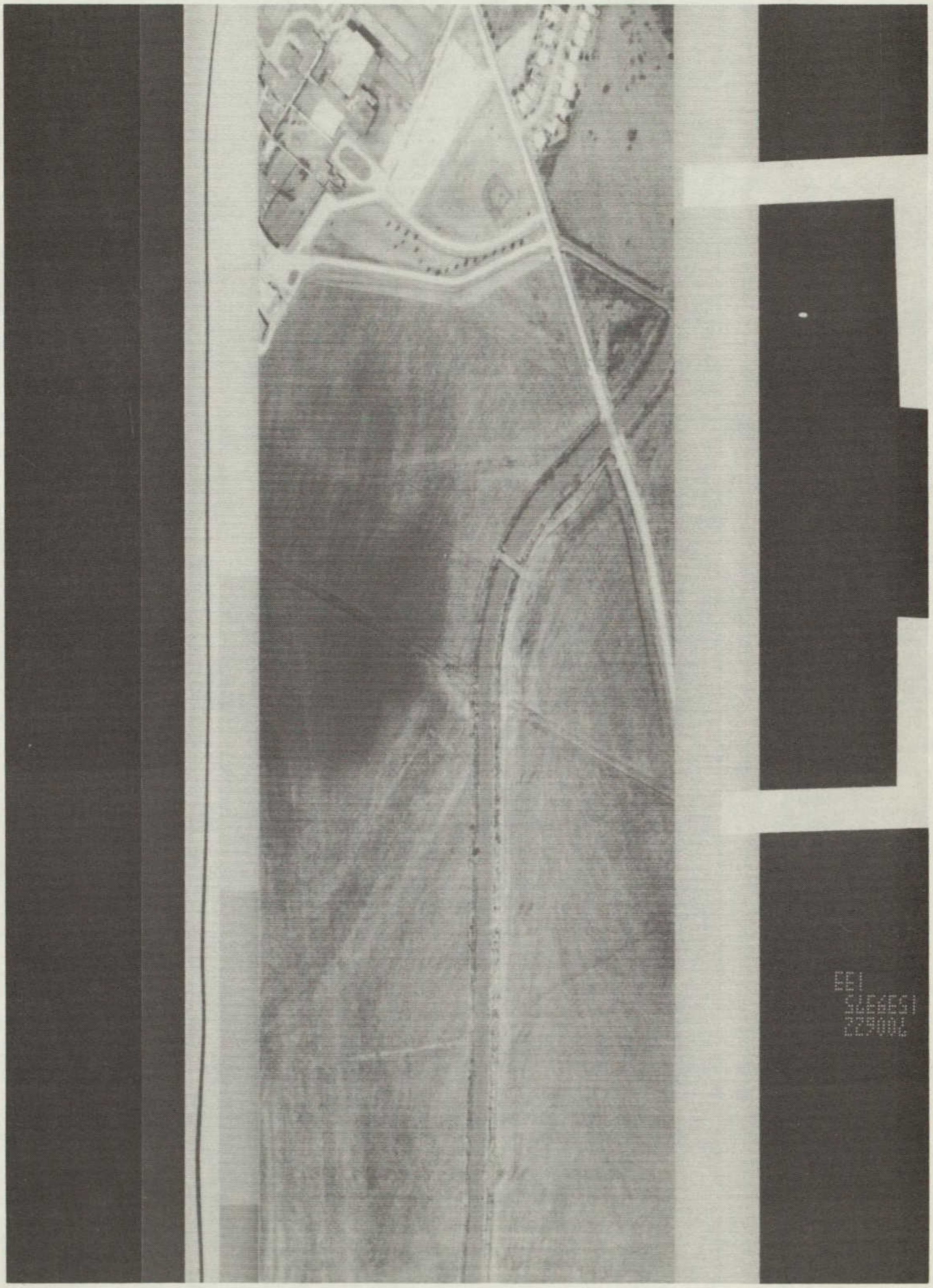

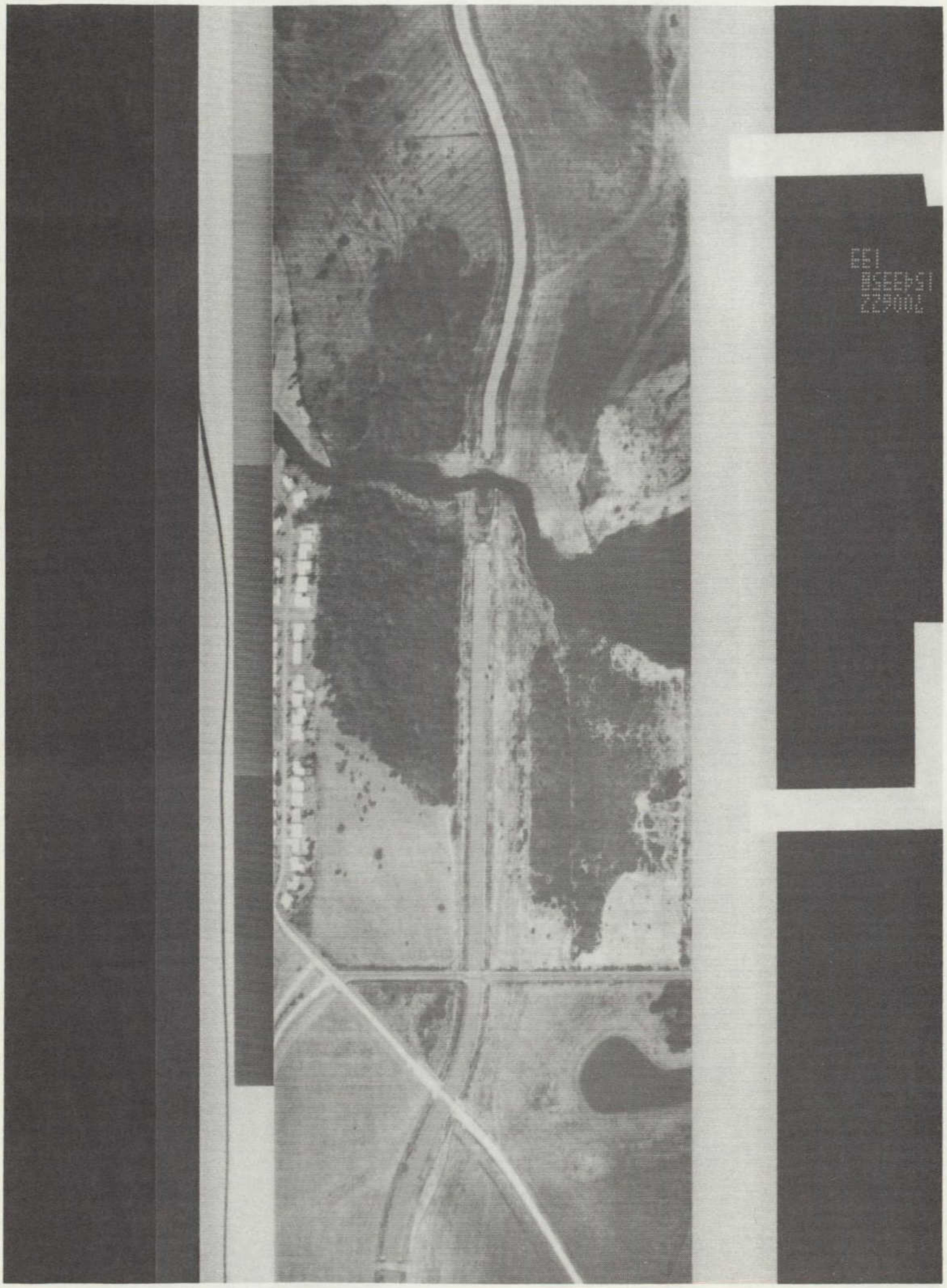

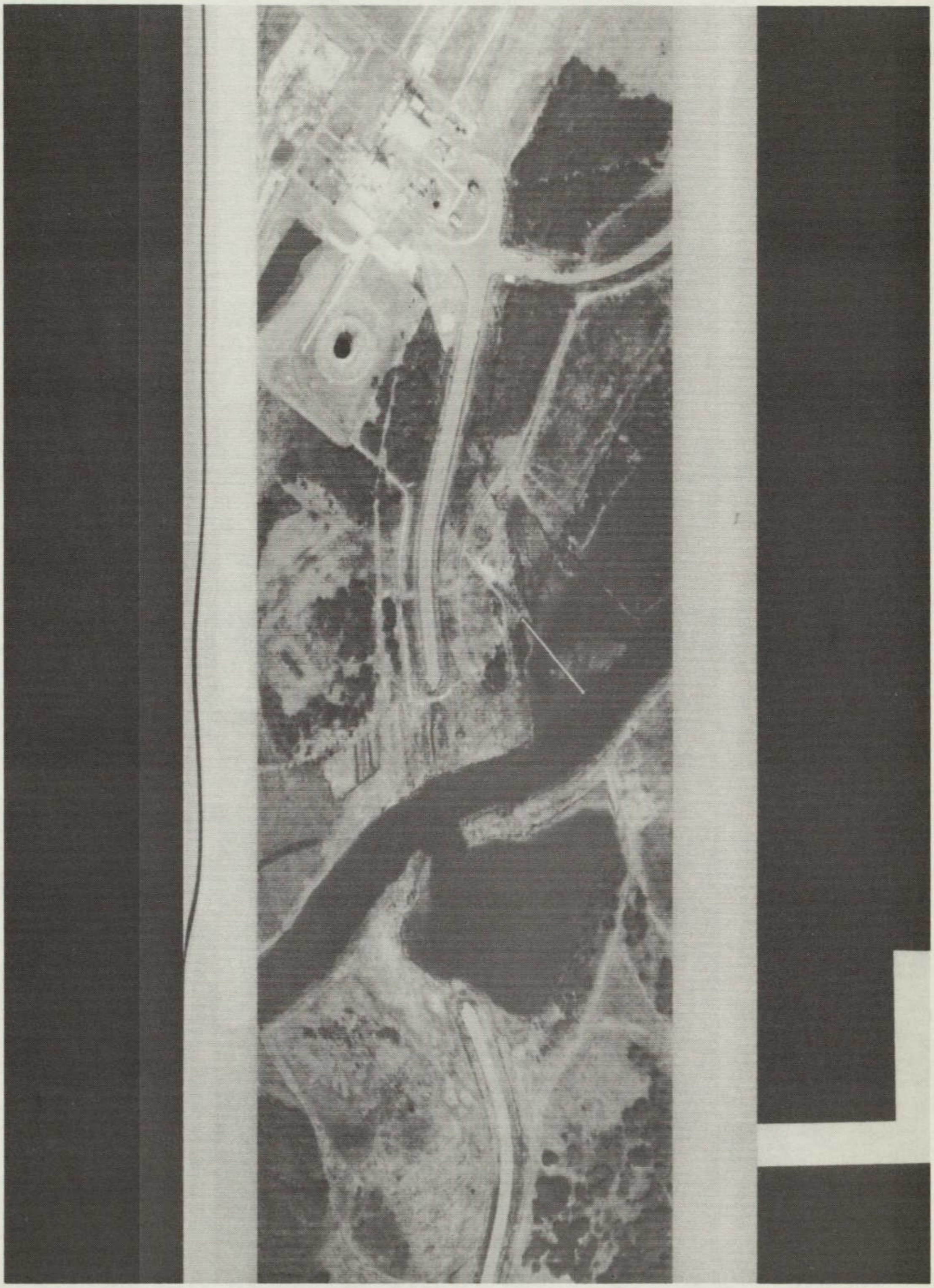

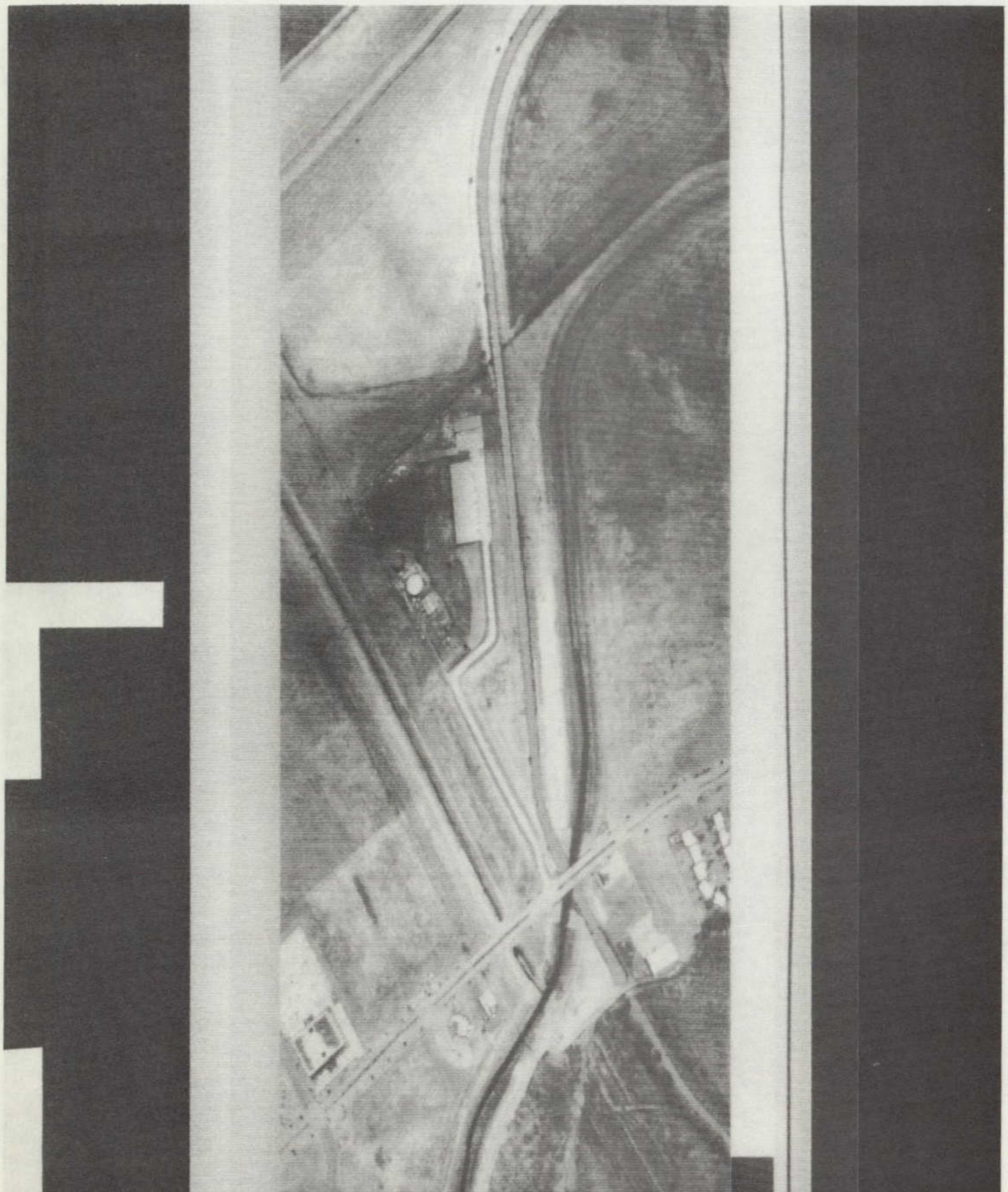

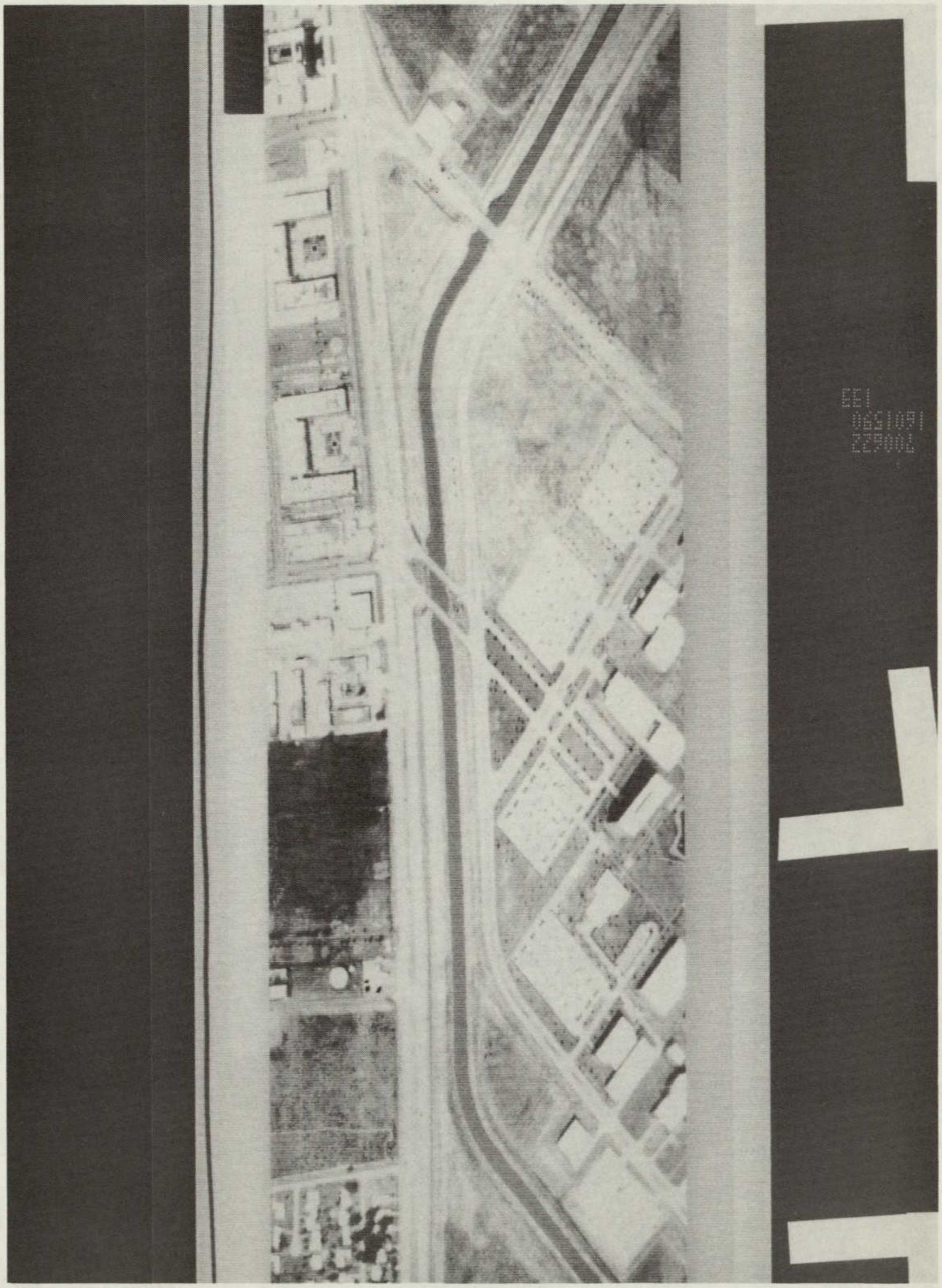

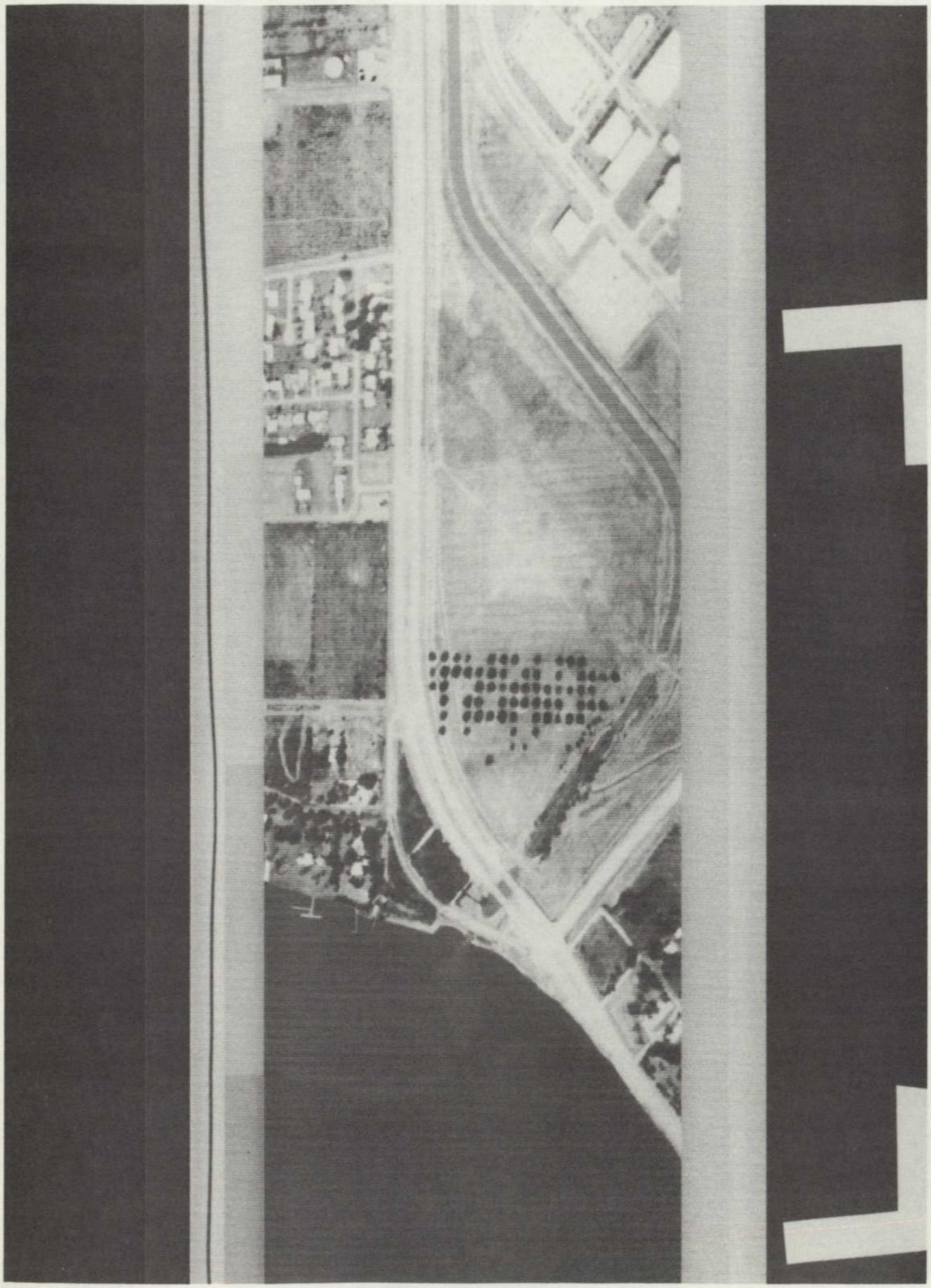

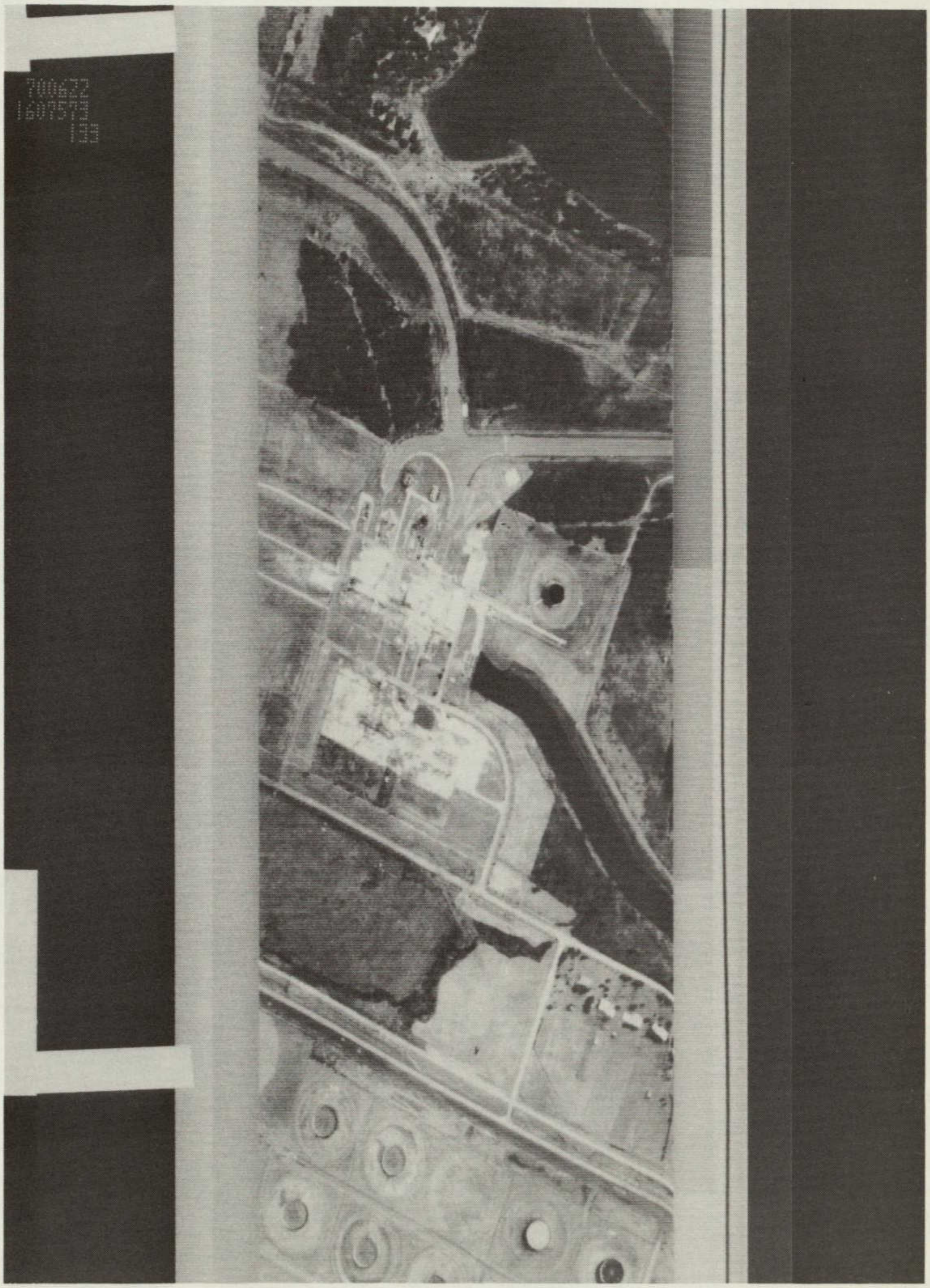

The REMOTE SENSING CENTER was established by authority of the Board of Directors of the Texas A&M University System on February 27, 1968. The CENTER is a consortium of four colleges of the University; Agriculture, Engineering, Geosciences, and Science. This unique organization concentrates on the development and utilization of remote sensing techniques and technology for a broad range of applications to the betterment of mankind.